AD-A044 176 AIR FORCE GEOPHYSICS LAB HANSCOM AFB MASS F/G 9/2
THE TREATMENT OF LATERAL BOUNDARY CONDITIONS IN LIMITED-AREA MO--ETC(U)
APR 77 R SHAPIRO

UNCLASSIFIED AFGL-TR-77-0092 NL

1 OF 1
ADA044176

END
DATE FILMED
10-77
DDC

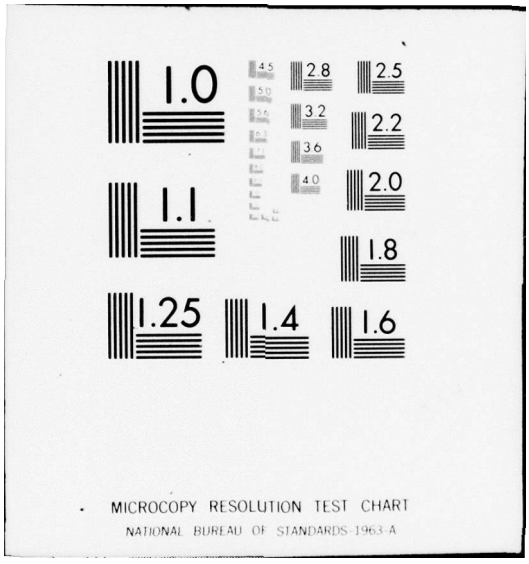
1.0
1.1
1.25
1.4
1.6
1.8
2.0
2.2
2.5
2.8
3.2
3.6
4.0
4.5
5.0
MICROCOPY RESOLUTION TEST CHART
NATIONAL BUREAU OF STANDARDS-1963-A

AFGL-TR-77-0092
ENVIRONMENTAL RESEARCH PAPERS, NO. 594

The Treatment of Lateral Boundary Conditions in Limited-Area Models: A Pragmatic Approach

RALPH SHAPIRO

19 April 1977

METEOROLOGY DIVISION PROJECT 2310
AIR FORCE GEOPHYSICS LABORATORY
HANSCOM AFB, MASSACHUSETTS 01731

AIR FORCE SYSTEMS COMMAND, USAF

This report has been reviewed by the ESD Information Office (OI) and is releasable to the National Technical Information Service (NTIS).

This technical report has been reviewed and is approved for publication.

FOR THE COMMANDER

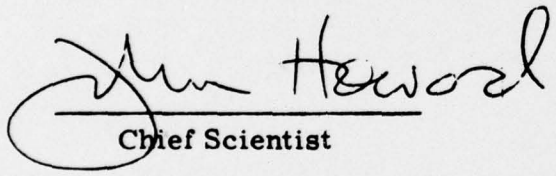

Chief Scientist

Qualified requestors may obtain additional copies from the Defense Documentation Center. All others should apply to the National Technical Information Service.

Unclassified

SECURITY CLASSIFICATION OF THIS PAGE (When Data Entered)

REPORT DOCUMENTATION PAGE	READ INSTRUCTIONS BEFORE COMPLETING FORM
1. REPORT NUMBER: AFGL-TR-77-0092, AFGL-ERP-594	3. RECIPIENT'S CATALOG NUMBER
4. TITLE (and Subtitle): THE TREATMENT OF LATERAL BOUNDARY CONDITIONS IN LIMITED-AREA MODELS: A PRAGMATIC APPROACH.	5. TYPE OF REPORT & PERIOD COVERED: Scientific, May 1976 - Apr 1977
	6. PERFORMING ORG. REPORT NUMBER: ERP No. 594
7. AUTHOR(s): Ralph Shapiro	8. CONTRACT OR GRANT NUMBER(s)
9. PERFORMING ORGANIZATION NAME AND ADDRESS: Air Force Geophysics Laboratory (LYD), Hanscom AFB, Massachusetts 01731	10. PROGRAM ELEMENT, PROJECT, TASK AREA & WORK UNIT NUMBERS: 61102F, 2310G201, G2
11. CONTROLLING OFFICE NAME AND ADDRESS: Air Force Geophysics Laboratory (LYD), Hanscom AFB, Massachusetts 01731	12. REPORT DATE: 19 April 1977
	13. NUMBER OF PAGES: 69
14. MONITORING AGENCY NAME & ADDRESS (if different from Controlling Office): Environmental research papers, May 76 - Apr 77	15. SECURITY CLASS. (of this report): Unclassified
	15a. DECLASSIFICATION/DOWNGRADING SCHEDULE

16. DISTRIBUTION STATEMENT (of this Report)

Approved for public release; distribution unlimited.

17. DISTRIBUTION STATEMENT (of the abstract entered in Block 20, if different from Report)

12 68p.

18. SUPPLEMENTARY NOTES

19. KEY WORDS (Continue on reverse side if necessary and identify by block number)

Initial-boundary value problem
High-order interpolation
Phase and amplitude restoration
High-order filter

20. ABSTRACT (Continue on reverse side if necessary and identify by block number)

Mathematical models used to simulate or predict atmospheric behavior are limited in scope because of insufficient knowledge of the initial conditions and forcing functions. But these limitations are generally dwarfed by the limited capacity and power of even the largest and most powerful computers. Thus, where a solution is required with high resolution for some limited area of interest, it is often impractical to solve the model throughout the entire domain with the same uniformly high resolution. A number of methods have been proposed for treating the mathematical and numerical problems that arise in the

DD FORM 1 JAN 73 1473 EDITION OF 1 NOV 65 IS OBSOLETE

Unclassified

SECURITY CLASSIFICATION OF THIS PAGE (When Data Entered)

409 578

20. (Cont)

boundary or transition region between the high and low resolution solutions. For any problem of practical interest there is no "correct" way of handling the boundary problems and no way of avoiding some boundary generated noise. Consequently a pragmatic approach is proposed here which overspecifies the artificial lateral boundaries of a fine-mesh, limited-area, nested region and depends upon a high-order phase and amplitude restoring interpolation along with a high-order, but weak, smoothing operator to control noise and ensure verisimilitude.

The basic problem as well as the method proposed is outlined in some detail in the Introduction. High order amplitude restoring and phase and amplitude restoring interpolation operators are defined and constructed in Section 2. In Section 3, both static and dynamic comparisons are made between the two types of interpolation operators. In the static tests, the phase and amplitude restoring interpolation is shown to be superior in minimizing root mean square differences between interpolated values and analytic values of simple Fourier functions.

The dynamic tests are carried out in the framework of a multilevel primitive equation model and show unequivocally the importance of correct phase information for the lateral boundaries of the fine-mesh region. The results obtained indicate that the simple procedure proposed here should yield satisfactory results in operational fine-mesh, limited-area models.

Preface

A considerable debt to Dorothy Moran is gratefully acknowledged for interpreting an unfamiliar program and shepherding the computations to completion with her customary skill and nerve. To Carmel Vermette I wish to convey my admiration for her unique ability in deciphering my script and her unsurpassed capacity in translating it to type.

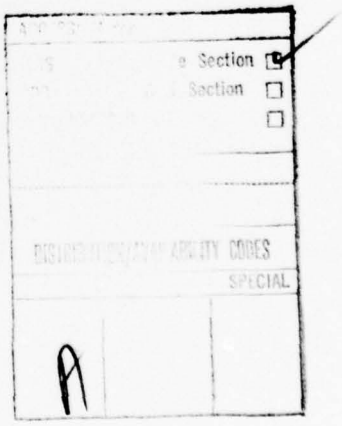

Contents

Illustrations

Tables

The Treatment of Lateral Boundary Conditions in Limited-Area Models: A Pragmatic Approach

1. INTRODUCTION

Routine prediction of atmospheric behavior, particularly the prediction of the gross features of the large-scale circulation, is commonly based upon the numerical solution of some mathematical model which is designed to incorporate the physics for those atmospheric features of immediate interest. The typical mathematical model consists of a set of nonlinear partial differential equations expressing the rate of change of momentum and heat (the prognostic equations) and an appropriate set of diagnostic equations expressing relationships among the prognostic variables and other variables which are required in the numerical solution of the prognostic equations.

The system is solved numerically as an initial value problem over a network of grid points in space. The distance between neighboring points in this network controls the detail that can be resolved in the predicted fields. However, though arbitrary to some extent, this distance is more or less determined by outside factors such as the scale size of the phenomena of interest, but especially by the available computer capacity. The required computer capacity is particularly sensitive to the grid distance since a halving of the mesh size in a three-space dimensional model increases the computer time by more than a factor of 10, assuming, optimistically, that the computer has sufficient unused internal (high speed) storage capacity to avoid a concomitant increase in the book-keeping operations.

(Received for publication 18 April 1977)

It is often desirable to increase the forecast resolution over some limited area of the globe where the observational density or the nature of the problem warrants increased resolution, but where economic factors make it impractical to increase the resolution uniformly over the whole globe. In fact, even if the machine capacity were available, it might be desirable in the interest of speed and economy to use a coarse-mesh resolution in regions where the fields are smooth and changing slowly and to use a fine-mesh resolution only in regions where the fields are changing rapidly in time and space. In such cases the problem no longer assumes the character of a pure initial value problem, but, depending upon the numerical procedure, assumes more or less the character of an initial boundary-value problem. There are a variety of ways in which such a problem can be handled.

(1) Perhaps the simplest is to choose the fine-mesh domain large enough so that during the course of the forecast the lack of knowledge of the boundary values cannot propagate into an interior region of interest and affect the value of the forecast in this interior region. This approach might be necessary if there were no information outside the boundary of the fine-mesh domain. Boundary errors are simply accepted and are kept under control by strong smoothing near the boundaries.[1] Inasmuch as this approach requires a large fine-mesh region it is computationally costly and in spite of its simplicity it is not generally used if there are reasonable alternatives.

(2) In the variable mesh approach a single solution is obtained for the 'global' domain, but the mesh density is allowed to vary so that regions of interest that warrant increased resolution are covered by a fine-scale mesh, whereas the remainder of the domain is covered by a coarse-scale mesh. The principal advantage of this approach is that there are no artificial lateral boundaries around the fine-mesh domain for which separate boundary conditions have to be specified. Furthermore, this approach permits a two-way interaction between the flow fields defined by the fine-and coarse-mesh regions.

This approach was used by Birchfield[2] in a moving coordinate system for a hurricane problem. Moretti[3] suggests a stretching transformation of the coordinates which has the virtue of permitting smooth transitions between the regions of different grid density. The variable mesh approach has been applied by Harrison and Elsberry[4] to a two-dimensional multilevel model and by Koss,[5] Ookochi,[6] and Phillips and Shukla[7] to the shallow-water equations. The variable mesh method was adopted by Mathur[8] in a four-level primitive equation hurricane model, while Price and MacPherson[9] discussed the use of cubic polynomial splines to fit the spatial variations of the dependent variables.

(Because of the large number of references cited above, they will not be listed here. See Reference Page No. 67, for References 1 through 9).

In spite of the advantages of this approach, as indicated above, the results have been generally disappointing except in cases where the large-scale domain fields tend to be smooth with weak gradients (such as in the hurricane problem), or where smoothness is ensured by the numerical technique (such as with the use of bicubic splines.[9] The inherent difficulty with the variable mesh approach arises from the fact that the phase speed of the waves is a function of the truncation error, which in turn depends upon the grid spacing as well as upon the dominant scale sizes of the field variables. Waves in the coarse-mesh domain will change phase speed when passing into the fine-mesh region and will interact, producing interference with the part of the wave that has remained in the coarse-mesh domain. As Browning et al[10] point out, this interference phenomenon is present regardless of the difference method used.

It seems intuitively apparent that abrupt changes in grid density would produce more serious interactions than a gradual, phased transition. Nevertheless, in view of the increased complexity in programming necessitated by this approach and in view of the dubious advantages (inasmuch as changes in grid density induce effects similar to those produced by artificial lateral boundaries,[11] it appears worthwhile to investigate a third general method.

(3) The third approach entails separate coarse-mesh and fine-mesh calculations, with the fine-mesh region nested within the coarse-mesh domain. The coarse-mesh solution is obtained for a 'global' domain without artificial lateral boundaries and serves to supply the necessary boundary information for a solution with a fine-mesh grid over a limited area of the globe. The principal difficulty with this approach concerns the choice of proper boundary conditions for the particular system of equations. This problem, while serious, appears amenable to treatment and the nested-domain approach seems fundamentally simpler for routine application than the variable-grid approach.

The choice of proper boundary conditions for the nested region has been extensively examined for simple, linearized hyperbolic systems.[12-14] The boundary conditions should provide a well-posed problem. That is, the solution should depend continuously upon the boundary data so that a small change in a boundary value

10. Browning, G., Kreiss, H.-O., and Oliger, J. (1973) Mesh refinement, Math. Comp., 27:29-39.

11. Kreiss, H.-O., and Oliger, J. (1973) Methods for the Approximate Solution of Time Dependent Problems, GARP Pub. Ser. No. 10, 103 pp.

12. Kreiss, H.-O. (1970) Initial boundary value problems for hyperbolic systems, Comm. Pure and Appl. Math., 23:277-298.

13. Gustafsson, B., Kreiss, H.-O., and Sundström, A. (1972) Stability theory of difference approximations for mixed initial boundary value problems, II. Math. Comp., 26:649-686.

14. Elvius, T., and Sundström, A. (1973) Computationally efficient schemes and boundary conditions for a fine-mesh barotropic model based on the shallow-water equations, Tellus, 25:132-156.

should have only an appropriately small effect on the solution. However, the non-viscous baroclinic primitive equations appear to be ill-posed for any specification of the lateral boundary conditions.[15] The difficulty, which is due at least in part to the hydrostatic approximation,[16] can be alleviated, if not overcome, by the expedient of an artificial viscosity.[11, 15] Additional boundary difficulties are introduced in solving the finite-difference equations, especially, when for purposes of reducing the truncation error, the finite-difference equations are of higher order than the original differential equations, thus requiring computational boundary conditions[17] and consequently giving rise to computational as well as physical solutions.[18]

Although unable to develop a general theory on the existence and uniqueness of solutions to nonlinear hyperbolic systems, Sundström[15] and Elvius and Sundström[14] discuss sufficient conditions for the well-posedness of the pure initial value problem for the shallow-water equations. For certain a-posteriori boundary conditions, the well-posedness also applies to the limited area problem (that is, to the initial-boundary value problem). Although it might appear reasonable to expect, it is not possible to state with confidence that for a given initial state the solution will remain continuous and differentiable.

In the case of the finite-difference equation for the limited-area problem, there remains even greater uncertainty. The stability of finite-difference solutions has been shown for simplified linear systems by the use of the energy method.[19, 20] For the general nonlinear limited-area problem Elvius and Sundström[14] suggest that the boundary conditions should be based upon their ability to control the growth of gravity wave disturbance rather than on their accuracy in describing the quasi-geostrophic part of the motion. In this connection they propose that only those boundary conditions that are required by the corresponding linearized system of differential equations should be specified a priori, and that the remaining (computational) boundary conditions should be obtained from the interior (and boundary) values of the limited area by some suitable interpolation (extrapolation) procedures This is essentially the approach that was first used by Charney et al,[21] however, as was subsequently shown by Platzman,[22] they used an inappropriate (unstable) extrapolation procedure for the outflow boundary points. To avoid the instability they abandoned the use of the 'proper' boundary conditions and resorted to simple over-specification with a smoothing procedure. For the primitive, barotropic shallow-water equations, Charney[23] argued on the basis of the characteristic quantities for the one-dimensional problem that similar boundary conditions are required; namely, the normal velocity should be specified at all boundary points and the potential vorticity at inflow points.

(Because of the large number of references cited above, they will not be listed here. See Reference Page No. 67, for References 15 through 23.)

Sundström[24] shows, by means of the energy method, that the barotropic vorticity equation in a confined region is properly posed with boundary conditions of the Charney-Fjörtoft-von Neumann[21] type (as well as other more general boundary conditions) for cases with open boundaries (that is, where no physical boundaries exist and the fluid flows in and out of the boundary region). With such proper boundary conditions, the solution is unique and convergent; that is, a small perturbation on the original solution will remain small and the solution is continuously dependent on the boundary conditions and initial data as long as certain derivatives of the solution remain bounded. Elvius and Sundström[14] propose three other sets of boundary conditions for this problem. In all three they specify the tangential velocity at inflow boundary points, so that the distinction among the three cases concerns the specification of an additional boundary condition for all boundary points. This second boundary condition determines the manner in which the gravity wave solutions will interact with the boundary. If the normal velocity is prescribed at the boundary, gravity waves are essentially trapped and reflected back into the limited area. If a combination of the normal velocity and the geopotential, corresponding to the ingoing characteristic for the gravity waves, is specified then a gravity wave approaching the boundary will pass out of the region without reflection and will be harmless. If on the other hand the geopotential itself is specified for the second boundary condition, this, like the first case, produces reflection of gravity waves. But while stable, though noisy, difference schemes have been devised for the first case, no stable difference scheme is known for the third case.

The number of additional (computational) boundary conditions (beyond those specified a priori) depends on the order of the difference equations. The additional conditions should not be specified, but should be determined from the boundary and interior values of the limited area by a method that is both accurate and stable.

In the final analysis Elvius and Sundström[14] assert that there is no easy, direct way of determining the stability properties of two- and three-dimensional difference schemes for limited area problems. The energy method has been used only for the case with boundary conditions that are open for external gravity waves. For other types of boundary conditions a method of stability analysis for initial-boundary value problems has been developed by Kreiss[25] and applied by Gustafsson et al,[13] but only for the one-dimensional case. Consequently, for any realistic problem, we are forced to rely on computer experimentation. In just such experiments, Elvius and Sundström[14] have obtained reasonable results with both the first and second types of boundary conditions; that is, where the tangential velocity is specified at inflow points and where either the normal velocity or a combination of normal velocity and geopotential is specified at outflow points. However, in those experiments

24. Sundström, A. (1969) Stability theorems for the barotropic vorticity equation, Mon. Wea. Rev., 97:340-345.

25. Kreiss, H.-O. (1971) Difference approximations for mixed initial boundary value problems, Proc. Roy. Soc. London, Ser A., 323:255-261.

where the initial data contains short as well as long waves, the results tended to be noisy. The primitive barotropic system of (shallow water) equations is a simple hyperbolic system which, by the use of the energy method, can easily be shown to be well-posed with such boundary conditions. However, the more realistic primitive system of equations, which describes a baroclinic, inviscid, dry, adiabatic and hydrostatic fluid, does not form a simple hyperbolic set of equations. Although the energy transfer equation has not been obtained for the linearized disturbance equations corresponding to this system, it has been obtained for a simplified system for which it can be shown that the pure initial value problem is well posed in that a small change in the initial conditions will remain small for all time as measured by a RMS norm.[15]

For the finite-difference formulation any difference between the prescribed boundary conditions and the correct boundary conditions will generate gravity waves and, although the errors may remain bounded, the solutions will be incorrect. If the differences between the prescribed and correct boundary conditions are large, nonlinear effects may generate real disturbances which could grow rapidly. A correct set of boundary conditions should specify the normal velocity and temperature in such a way that the outward propagating components are not hindered in passing out of the region. While it might be practicable to do this by using the phase speed of a single principal component in a Sommerfeld radiation boundary condition (as suggested by Pearson[26]), it is not practicable for a multilevel model possessing several eigenfunctions. To overcome this difficulty Orlanski[27] suggests a modification of the Sommerfeld radiation condition in which rather than a single constant phase velocity, a separate phase velocity is obtained for each variable from the grid point values in the vicinity of the boundary. This approach, which involves a certain amount of inherent smoothing has not been adequately tested. Instead Sundström[15] proposes to compromise the correctness of the boundary conditions for the multilevel model by using boundary conditions that are appropriate for the shallow water equation, that is, to prescribe the tangential velocity at inflow points and compute it at outflow points by a suitable extrapolation from the interior. In addition, the combination of the normal velocity and temperature corresponding to the first inward external gravity wave is prescribed everywhere and the combination corresponding to the first outward external gravity wave is computed by extrapolation. These are approximately the barotropic parts of the normal velocity and temperature. Finally the remaining baroclinic part of the normal velocity and temperature is specified at all boundary points. These conditions are admittedly an overspecification which permits the propagation and reflection of internal gravity-wave disturbances into

26. Pearson, R.A. (1974) Consistent boundary conditions for numerical models of systems that admit dispersive waves, J. Atmos. Sci., 31:1481-1489.

27. Orlanski, I. (1976) A simple boundary condition for unbounded hyperbolic flows, J. Comp. Phys., 21:251-269.

the region. Sundström[15] satisfies himself with the hope that the difficulties created by the internal gravity waves will be much less than those which could be generated by external gravity waves and that their effect can be diminished further by adding a diffusion term to the equation near the boundary zone.

It is apparent that, even if it were possible to define the "correct" boundary conditions for a realistic baroclinic limited-area problem, in practice the boundary conditions would at the very least contain truncation errors inasmuch as they would be determined not from continuous fields but from a small number of point values. However, in reality the boundary errors will be more severe in the finite-difference solution since the proper boundary conditions cannot be defined for realistic problems and at best one can apply boundary conditions which are appropriate for much simpler problems. Nevertheless, even for the simpler shallow-water problem, obtaining the proper boundary conditions is likely to involve computational and programming complexities. In this connection, Williamson and Browning[28] use a relatively simple set of lateral boundary conditions for the NCAR limited-area model. Following the approach of Shapiro and O'Brien[29] who worked with the nondivergent barotropic vorticity equation, Williamson and Browning[28] specify u, v, and t on points determined as inflow points from the global model solution. At outflow points they determine these parameters by interpolation from the fine-mesh solution, by determining the interior point which would have been the starting point of a parcel following a trajectory determined from the coarse-mesh flow field. As would be expected their results show appreciable two-grid-interval noise, but the noise does not appear to interfere with the definition of the large-scale fields. Nevertheless, they find it expedient to apply additional smoothing in a band of several grid intervals around the boundary of the limited area.

Davies[30,31] makes use of the energy method to establish criteria of uniqueness, which he then uses to determine boundary conditions for the barotropic shallow water equations as well as for the baroclinic primitive equations. However, these conditions have been criticized for overspecification by DeRivas[32] as well as by Sundström.[15] Recently, Davies[33] has proposed a different procedure. Starting

28. Williamson, D. L., and Browning, G. L. (1974) Formulations of the lateral boundary conditions for the NCAR limited-area model, J. Appl. Meteor., 13:8-16.

29. Shapiro, M. A., and O'Brien, J. J. (1970) Boundary conditions for fine-mesh limited-area forecasts, J. Appl. Meteor., 9:345-349.

30. Davies, H. C. (1973a) On the lateral boundary conditions for the primitive equations, J. Atmos. Sci., 30:147-150.

31. Davis, H. C. (1973b) On the initial-boundary value problem of some geophysical fluid flows, J. Comp. Phys., 13:398-442.

32. DeRivas, E. K. (1974) Comments "On the lateral boundary conditions for the primitive equations," J. Atmos. Sci., 31:596.

33. Davies, H. C. (1976) A lateral boundary formulation for multi-level prediction models, Quart. J. Roy. Met. Soc., 102:405-418.

from the position that in all practical applications (in the one-way interaction limited area problem) the available boundary data will contain inherent errors, he proposes an expedient method involving the relaxation of the interior flow in the vicinity of the boundary to the external fully prescribed flow. The method reduces the sensitivity of the governing equations to overspecifications of the boundary data and achieves a reduction in the noise generation at the lateral boundaries by means of an artificial modification of the equations. The modification consists of a Newtonian-type adjustment term with a relaxation coefficient whose spatial dependence is such as to force the interior field values to approach the specified boundary values in a smooth fashion. The method has the virtue of simplicity and seems to be effective for the single test cases shown; however, it is not obvious to what physical problem the adulterated equations apply. While it is apparent that the method induces a certain amount of smoothing between the specified boundary values and the interior fine-mesh values the total smoothing function does not have a single amplitude response function (because of the spatial variation in the relaxation coefficient) and therefore it is not possible to assess the extent of the smoothing involved.

That some form of smoothing might be necessary can be inferred from the recent comments of Bennett.[34] He asserts that suitable open boundary conditions at the outflow points of a limited area (that is, boundary conditions which avoid trapping computational noise in the limited forecast area) are possible only for small amplitude, short wavelength, barotropic waves; that "noise problems are unavoidable in planetary or baroclinic wave forecasts."

On the assumption that for realistic, three-dimensional problems a certain amount of boundary error is inevitable (regardless of the choice of boundary conditions and the method used to obtain them) a high-order interpolation procedure was proposed[35] for supplying time-dependent boundary values in a fine-mesh limited-area model. The interpolation was performed on a 'global' coarse-mesh solution which was run concurrently with, but independent of, the fine-mesh solution. The aim of this experiment was to determine whether the use of a high-order interpolation (eight points in one dimension), which was designed to represent faithfully the amplitudes of all waves except the very short waves,[36] would produce a smooth transition between the specified boundary values and the calculated, interior fine-mesh values. Numerical simulation experiments were carried out in a nested

34. Bennett, A. F. (1975) Open Boundary Conditions for the Limited Area Forecasting Problem, Report No. 9, The GARP Programme on Numerical Experimentation, A. Robert, Ed., pp 114-115

35. Shapiro, R. (1973) A High-Order Interpolation Procedure for Use in Fine-Mesh Limited-Area Models, Phys. Sci. Res. Pap., No. 560, AFCRL-TR-73-0543, 24 pp.

36. Shapiro, R. (1972) Information loss and compensation in linear interpolation, J. Comp. Phys., 10:65-84.

region with a grid spacing one-fifth the size of the coarse grid length within the framework of an eight-level, dry, inviscid, primitive-equation model. Boundary information was supplied from the coarse-mesh solution by interpolation for all prognostic variables for all of the fine-mesh boundary points, regardless of whether the flow was in or out of the limited area. This is obviously an overspecification of the boundary conditions, but, as shown by Chen and Miyakoda,[37] such overspecification has the advantage of simplicity and with smoothing gives results comparable to those obtained with presumably well-posed boundary conditions.

In the above-mentioned study[35] a comparison was made between two methods of interpolation from the coarse-mesh solution, a linear and a high-order interpolation. The high-order interpolation procedure is strongly damping for two- and three-grid interval waves, but barely has any effect on waves longer than about six grid lengths even after many applications of the operator.[36] The linear interpolation is at least as strongly damping for short waves as the high-order interpolation, but more importantly, the linear interpolation is strongly damping for even moderately long waves.

The solutions obtained with the use of high-order interpolation, although by no means noise-free, were noticeably smoother than those obtained with linear interpolation. The latter solutions were seriously contaminated with noise. Since there was no viscous dissipation in the model, a weak smoothing operation was applied to the coarse-mesh solution every ten time steps (every 200 min). This same smoothing was also applied to each fine-mesh solution every 200 min (every 50 time steps). In view of the weakness of the smoothing operation, the relative smoothness of the solution with high-order interpolation was striking. It was felt that the remaining roughness of these solutions could be controlled by a combination of more frequent smoothing and by using an interpolation procedure which not only is efficient in restoring wave amplitudes damped by linear interpolation, but also minimizes phase error. The present study describes an attempt to remove the remaining roughness by such means, using the same basic model framework and maintaining the same simple overspecified boundary conditions.

A modification of the high-order interpolation procedure used in the earlier study was made which, while still maintaining the amplitude-restoring properties, minimizes the phase error arising from interpolation. A new series of fine-mesh limited-area solutions is carried out in which comparisons are made among three methods of interpolating the coarse-mesh solution onto the limited-area boundaries: linear interpolation, high-order amplitude restoring interpolation, and high-order phase and amplitude restoring interpolation. In addition, solutions are obtained with differing frequencies of smoothing in order to test the relative importance of

37. Chen, J.H., and Miyakoda, K. (1974) A nested grid computation for the barotropic free surface atmosphere, Mon. Wea. Rev., 102:181-190.

the smoothing and interpolation operations. The aim of these experiments is the development of a simple, practical procedure for solving a multilevel primitive equation model over a limited area with fine mesh resolution without the need for solving the global model with a fine-mesh grid. We therefore propose to specify all prognostic variables at all boundary points. We justify this overspecification of the boundary conditions on the basis that:

(1) The proper boundary conditions can be shown only for simplified linear systems.

(2) Even if we knew the proper boundary conditions for realistic, three-dimensional nonlinear problems, we would have to specify some of the boundary conditions in the finite-difference solution from the outside region, where at best the values are known less accurately. Consequently, boundary errors are inevitable in practice.

(3) Since we do not know the proper boundary conditions and cannot eliminate boundary errors completely, some kind of artificial smoothing is necessary.

(4) In view of the availability of simple and highly effective smoothing and filtering procedures which can be designed to be as scale-dependent as desired,[38,39] and in view of the results of Chen and Miyakoda[37] with overspecified boundary conditions, it is felt worthwhile to avoid the complexities of attempting to approximate proper boundary conditions and adapt the simple expedient of overspecification and filtering.

2. INTERPOLATION

The process of interpolation is widely used to obtain estimates of parameters at certain points in time or space from known or measured values which are available only at other points. It is tacitly assumed, when using interpolation, that the parameter has a value at the point in question. It is also assumed that the value of the parameter at any desired point may be estimated from some function of the known or given values of the parameter. In effect, it is assumed that the sample of the known set of values is representative of the entire field. If we make explicit what is usually implicit in any event, namely that the parameter is continuous over the domain, we may speak of its Fourier spectrum. In particular, we consider the discrete, finite Fourier representation of the field which is obtained from the set of values at known points to contain all of the available information concerning the field and that the best estimate of the value of the parameter at the point in question is that which is derived from this Fourier representation of the known field. Using

38. Shapiro, R. (1970) Smoothing, filtering, and boundary effects, Rev. Geophys. and Space Phys., 8:359-387.

39. Shapiro, R. (1975) Linear filtering, Math. Comp., 29:1094-1097.

this measure of best estimate, the author[36] proposed an interpolation operator which compensates for the Fourier amplitude truncation produced by two-point linear interpolation. The aim of this report is to generalize the operator and to propose a specialized procedure which minimizes phase as well as amplitude truncation.

2.1 Amplitude Restoration

Following the procedure adopted earlier,[39] let f(x) represent some function of time or space in one dimension, integrable in the finite domain $-D < x < D$, and let $f(x_i) = f_i$ for discrete values of x such that $x_i = i\Delta x$, where i is an integer and $\Delta x > 0$ is such that $2D/\Delta x$ is an integer. Two-point linear interpolation at the point $i = r\Delta x$, where $0 \leq r \leq 1$, is defined by

$$f^{(0)}_{i+r} = r f_{i+1} + (1 - r) f_i , \tag{1}$$

where the interval (-D, D) has been scaled so that $\Delta x = 1$.

Then f_i can be expressed in terms of a sum of Fourier components of the general form $A_n \sin(nx_i + \varphi_n)$, where A_n is the amplitude of the wave component with wave number n ($n = 2\pi/\lambda$, where λ is the wavelength of the component), and φ_n is the phase of the component; f_{i+r}, the value of the function at the point i+r can be similarly represented by a sum of components of the form $A_n \sin\left[n(x_i + r\Delta x) + \varphi_n\right]$ and the corresponding interpolated value, $f^{(0)}_{i+r}$ by components of the form

$$A^{(0)}_n \sin\left[n(x_i + r\Delta x) + \varphi_n - d_n\right] , \text{ where}$$

$$A^{(0)}_n = \left[1 - 4\, r\,(1 - r) \sin^2 \frac{n\Delta x}{2}\right]^{1/2} A_n , \tag{2}$$

and where

$$d_n = \tan^{-1} \left\{ \frac{(1-r) \sin nr\Delta x - r \sin\left[n\,(1 - r)\,\Delta x\right]}{(1-r) \cos nr\Delta x + r \cos\left[n\,(1 - r)\,\Delta x\right]} \right\} ; \tag{3}$$

$A^{(0)}_n / A_n = \rho^{(0)}_n$ expresses the amplitude damping, and d the phase shift, produced by two-point linear interpolation. It is apparent that two-point linear interpolation can introduce considerable damping of amplitude and shifting of phase, especially for the higher wave number components. For wave numbers greater than zero (omitting the cases where $r = 0$ or 1 for which $f^{(0)}_{i+r} = f_{i+r}$), $d = 0$ only if $r = 0.5$. It is also apparent from (3) that $d(r) = -d(1 - r)$.

The value of r (or 1 - r) for which the magnitude of d is a maximum is a function of n and can easily be determined from (3). For waves equal to or longer than 3-grid intervals, this value of r is near 0.25. It varies from 0.2666 for 3-grid interval waves to 0.2113 for infinitely long waves. For the 2-grid interval wave, Eq. (3) reduces to $d = \pi r$, except for $r = 0$, 1/2, or 1, for which $d = 0$. Thus, for the

2-grid interval wave, there is a discontinuity in d at r = 0.5. For all longer waves, d is continuous.

It has been shown[36] that the inverse of $\rho_n^{(0)}$ for all values of t and a (except for $t \sin^2 a = 1$ for which there is no inverse) is given by the infinite series

$$\left[\rho_n^{(0)}\right]^{-1} = 1 + \frac{t}{2}\sin^2 a + \frac{1.3}{2.4}t^2 \sin^4 a + \frac{1.3.5}{2.4.6}t^3 \sin^6 a + \\ + \ldots + \frac{1.3.5. \ldots (2h-1)}{2.4.6. \ldots (2h)} t^h \sin^{2h} a + \ldots , \qquad (4)$$

where $t = 4r(1 - r)$ and $a = n\Delta x/2$. Then $t \sin^2 a = 1$ occurs only for the $2\Delta x$ wavelength with r = 0.5. This wavelength, the shortest Fourier component that can be resolved with the given data, is completely eliminated by two-point linear interpolation when r = 0.5.

The series (4) is a monotonically increasing function of h. If we operate on $f_{i+r}^{(0)}$ with an operator representing a truncation of the series (4), we can (with the exception noted above) restore the amplitudes of the various Fourier components which had been damped by two-point linear interpolation. We note that $\sin^2 a$ is the Fourier representation of the operator $(-\delta^2/4)$ where $\delta(\ )_i = (\ )_{i+1/2} - (\ )_{i-1/2}$. That is, operating on any function with $(-\delta^2/4)$ is equivalent to multiplying the amplitude of the component with wave number n by $\sin^2 a$.

$$\delta^2(\ )_i = (\ )_{i+1} - 2(\ )_i + (\ )_{i-1} . \qquad (5)$$

Thus, the series (4) can be represented as the operator:

$$\left[\rho_n^{(0)}\right]^{-1} = 1 + 1/2\left(\frac{-t}{4}\delta^2\right) + \frac{1.3}{2.4}\left(\frac{-t}{4}\delta^2\right)^2 + \ldots + \frac{1.3.5 \ldots (2h-1)}{2.4.6 \ldots (2h)}\left(\frac{-t}{4}\delta^2\right)^h \\ + \ldots . \qquad (6)$$

It is apparent that the operator defined by (6) operating on $f_{i+r}^{(0)}$ is linear (additive), in that each term of the series consists of a centered symmetrical operation involving two grid points additional to the next lower ordered term. Thus, the interpolation operator of 2 (h + 1) points in one dimension consists of the operator defined by the series (6) truncated at the hth term, operating upon $f_{i+r}^{(0)}$. This operator differs from the operator discussed in Shapiro[36] which is multiplicative and less efficient. It is apparent that this operator, which we can write as

$$f_{i+r}^{(h)} = \left[1 + 1/2\left(\frac{-t}{4}\delta^2\right) + \frac{1.3}{2.4}\left(\frac{-t}{4}\delta^2\right)^2 + \frac{1.3.5. \ldots (2h-1)}{2.4.6. \ldots (2h)}\left(\frac{-t}{4}\delta^2\right)^h\right] f_{i+r}^{(0)} ,$$

has an amplitude response which, in the limit as h approaches infinity, approaches $(1 - t \sin^2 a)^{-1/2} (1 - t \sin^2 a)^{1/2} = 1$. Furthermore, we shall show, for any value of h, the amplitude response is a maximum.

For any level of restoration h, and any function F_j, $f^{2h}F_j$ is a linear combination of $(2h + 1)F_k$, $k = j, j \pm 1, \ldots, j \pm h$, given by

$$\delta^{2h} F_j = (-1)^h \binom{2h}{h} F_j + \sum_{k=0}^{h-1} (-1)^k \binom{2h}{k} \left[F_{j+(h-k)} + F_{j-(h-k)} \right] , \tag{7}$$

where $\binom{n}{m}$ are the binomial coefficients. Thus (6) truncated at the level h, may be written as an operator on F_j

$$\begin{aligned} R^{(h)}(F_j) = F_j + 1/2 \left(\frac{-t}{4}\right) \left[-2F_j + F_{j+1} + F_{j-1} \right] \; + \\ + \frac{1.3}{2.4} \left(\frac{-t}{4}\right)^2 \left[6F_j - 4 \left(F_{j+1} + F_{j-1} \right) + F_{j+2} + F_{j-2} \right] \; + \\ + \frac{1.3.5}{2.4.6} \left(\frac{-t}{4}\right)^3 \left[-20F_j + 15 \left(F_{j+1} + F_{j-1} \right) - 6 \left(F_{j+2} + F_{j-2} \right) + \right. \\ \left. + F_{j+3} + F_{j-3} \right] + \ldots + \frac{1.3.5. \ldots (2h-1)}{2.4.6. \ldots (2h)} \left(\frac{-t}{4}\right)^h \left[(-1)^h \binom{2h}{h} F_j \right. \\ \left. + \sum_{k=0}^{h-1} (-1)^k \binom{2h}{k} \left(F_{j+(h-k)} + F_{j-(h-k)} \right) \right] \; . \end{aligned} \tag{8}$$

If F_j represents two-point linear interpolation, $f^{(0)}_{i+r}$, then $R^{(h)}(F_j) = f^{(h)}_{i+r}$ is an interpolation operator which, at the level of restoration, h, maximizes the restoration of amplitude damped by $f^{(0)}_{i+r}$. That is, the interpolation operator defined by (8) operating on $f^{(0)}_{i+r}$ is ideal in the sense that for any linear operator involving $2(h + 1)$ points it maximizes the restoration of amplitude damped by two-point linear interpolation.

The property of maximum restoration can be demonstrated by induction. Using Eqs. (2) and (4), we write the amplitude response function for the hth level of restoration as:

$$\begin{aligned} \rho_n^{(h)} = \rho_n^{(0)} \left[1 + \frac{t}{2} \sin^2 a + \frac{3}{8} t^2 \sin^4 a + \ldots + \right. \\ \left. + \frac{1.3.5. \ldots (2h-1)}{2.4.6. \ldots (2h)} t^h \sin^{2h} a \right] \; . \end{aligned}$$

Then we write amplitude response function for the $(h + 1)$th level of restoration as

$$\rho_n^{(h+1)} = \rho_n^{(0)} \left[1 + \frac{t}{2} \sin^2 a + \ldots + \frac{1.3.5. \ldots (2h-1)}{2.4.6. \ldots (2h)} t^h \sin^{2h} a + \right.$$

$$\left. + A t^{h+1} \sin^{2(h+1)} a \right] .$$

We solve for A under the condition that $d\rho_n^{(h+1)}/dh = 0$ and $\rho_n^{(h+1)}$ is a maximum and find that

$$A = \frac{1.3.5. \ldots (2h+1)}{2.4.6. \ldots (2h+2)} ,$$

which is the coefficient of $t^{h+1} \sin^{2(h+1)} a$ in the series (4).

Inasmuch as the general term in (8)

$$\frac{1.3.5. \ldots (2h-1)}{2.4.6. \ldots (2h)} = \frac{(2h)!}{[2h.(2h-2). \ldots 6.4.2]^2}$$

$$= \frac{(2h)!}{2^{2h}(h!)^2} = \frac{1}{2^{2h}} \binom{2h}{h} ,$$

with the aid of (7), (8) can be expressed in compact form

$$R^{(h)}(F_j) = \sum_{h=0}^{h} \left\{ \frac{(t/4)^h}{2^{2h}} \binom{2h}{h}^2 F_j + \frac{(-1)^h (t/4)^h \binom{2h}{h}}{2^{2h}} \sum_{k=0}^{h-1} (-1)^k \binom{2h}{k} \times \right.$$

$$\left. \times \left[F_{j+(h-k)} + F_{j-(h-k)} \right] \right\} . \qquad (9)$$

Similarly, the amplitude response function corresponding to the amplitude-restoring interpolation operator (9) is

$$\rho_n^{(h)} = \rho_n^{(0)} \sum_{h=0}^{h} \binom{2h}{h} (t/4)^h \sin^{2h} a ,$$

where $\rho_n^{(0)}$ is the amplitude response function corresponding to the operator F_j in (9). In all applications in this paper F_j represents two-point linear interpolation at the point $j = i + r$. Thus, $R^{(h)}(F_j) = f_{i+r}^{(h)}$ in any application.

Figure 1 demonstrates the efficiency of (9) as an amplitude restoring interpolation operator for various values of h for the case where r = 0.5, for which the amplitude error is a maximum for any given h. The values of h range from 0, which corresponds to two-point linear interpolation, to 8, which corresponds to an 18-point interpolation operator. The amplitude response of each operator, represented as P_h in Figure 1, is shown as a function of wave number determined from 72 equally spaced grid points. Wave number 36, therefore, corresponds to a wavelength of $2\Delta x$, twice the grid distance. Since the two-grid interval wave is eliminated by two-point linear interpolation when r = 0.5, the amplitude of this wave remains zero for all h. The ordinate scale in Figure 1 is linear from 0.0 to 0.9 and logarithmic

above 0.9. Since fractional wave numbers have no meaning, the curves connecting the points for each operator have been drawn to assist in the interpretation of the figure. The curves are not joined for points on opposite sides of the 0.9 dividing line to emphasize the change of scale.

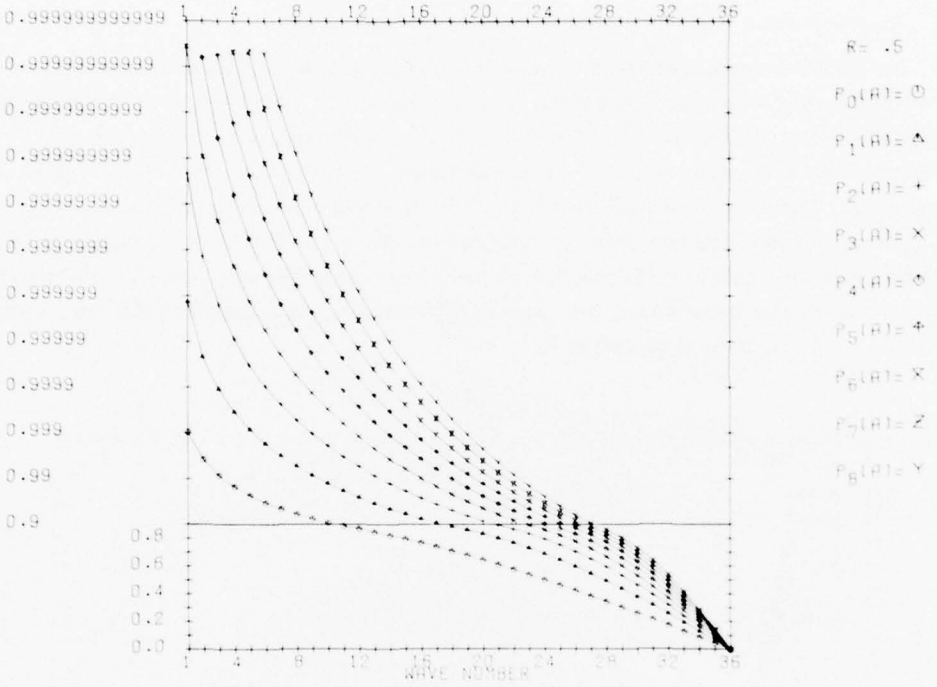

Figure 1. The Amplitude Response of the Amplitude Restoring Interpolation Operator, Eq. (9), as a Function of Wave Number in a 72-Point Periodic Domain. The operator is represented as P_h where h indicates the order of restoration. The ordinate scale is linear from 0.0 to 0.9 and logarithmic for higher values

It is apparent from Figure 1 that there is almost complete restoration of the amplitudes of the longer waves even for relatively low values of h. For values of $h \geq 3$, there is very little damping of waves longer than 3-grid intervals (wave number 24). For example, the amplitude of the 3-grid-interval wave for h = 4 is 0.902, as compared with its value for h = 0 of 0.500, and for the 4-grid-interval wave (wave number 18), the comparable values are 0.990 and 0.707. Since the damping is a maximum for r = 0.5, the restoration of amplitude for any h is somewhat more complete for other values of r than that shown in Figure 1. For any given r, the

restoration of amplitude is a function only of h and wave number; consequently, the most suitable level of restoration can be selected for a particular application. However the ability of an interpolation operator to approximate a given function depends upon phase error as well as amplitude error. Therefore we shall consider the merits of an interpolation operator which minimizes both amplitude and phase error.

2.2 Phase Restoration

As we have seen, two-point linear interpolation not only damps the amplitude of each Fourier component but also, in general, shifts the phase of each component. Figure 2 shows the phase difference, d, [Eq. (3)] in radians as a function of r, as well as -d as a function of (1 - r) in parentheses, for waves longer than 3-grid intervals. The only exception to phase shifting occurs when the interpolation point is midway between the two data points; that is, when r = 0.5. This feature of two-point linear interpolation for r = 0.5 permits the definition of a special interpolation procedure for the case where the ratio of the original grid length to the final interpolation grid length is a power of 2.

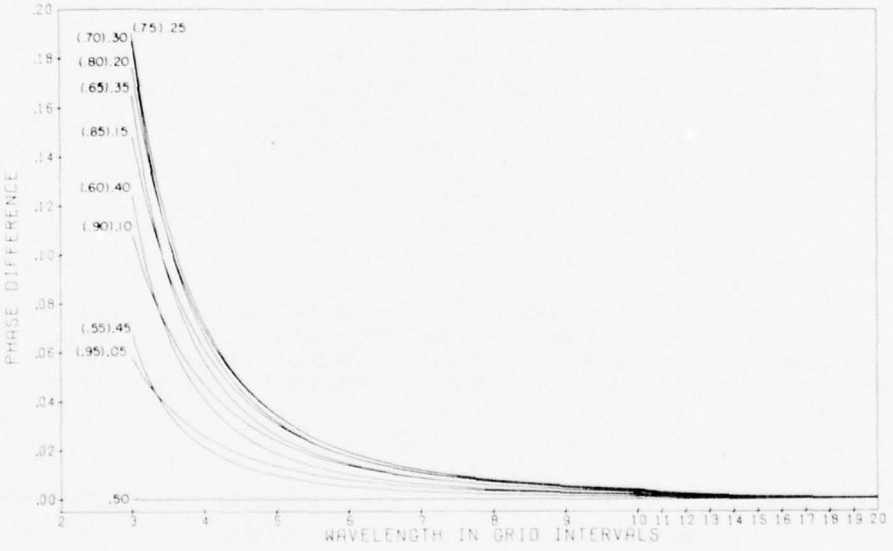

Figure 2. The Phase Difference, d or (-d), in Radians for Two-Point Linear Interpolation as a Function of Wavelength in Grid Intervals for Various Values of r or (1-r)

If we apply two-point linear interpolation [Eq. (1)] with r = 0.5 throughout the domain, we obtain values of the parameter at a set of discrete points consisting of

original data points and interpolated data points situated midway between the original points. Since no phase shift has been introduced by this interpolation procedure, we may correct for the amplitude truncation by applying the high ordered amplitude restoring operator (9) at some suitable level of truncation, say h = q. After applying (9), the set of original and interpolated data has virtually the same spectral properties as the original data except for the disappearance of the 2-grid-interval wavelength. Since the true $2\Delta x$ wave is likely to be poorly represented in the original data and troublesome in computations because it is often strongly contaminated by noise, it is frequently advantageous to eliminate it from the original data. Therefore, the suppression of the $2\Delta x$ wave is a desirable and advantageous feature of the interpolation operator. The set of combined original data and interpolated data with restored amplitude may be considered as a new set of homogeneous data with values given at grid intervals $\Delta x/2$. The above procedure can now be repeated, to obtain in turn, other sets of homogeneous data with values at grid intervals $\Delta x/4$, $\Delta x/8$, ... $\Delta x/2^m$. This process can be expressed formally as follows:

We define a variable position point α and an interim grid interval Δx^* such that $\alpha = i + p\,\Delta x/2^{m+1}$ and $\Delta x^* = \Delta x/2^M$ where m = 0, 1, 2, ... , M and where p = 1, 3, 5, ... , $(2^{M+1})-1$. It is apparent that α represents a special class of position points i + r* between i and i + 1 where r* assumes only the values of 1/2 (for m = 0); 1/4 and 3/4 (for m = 1); 1/8, 3/8, 5/8, and 7/8 (for m = 2); and so forth. It is also apparent that this phase and amplitude restoring interpolation operator may be expressed in terms of the amplitude restoring operator (9), as,

$$f_{\alpha}^{(h,q)} = R^{(h)}\left(F_{\alpha}^{(q)}\right) = R^{(h)}\left[\,1/2\left(f^{(q)}_{\alpha+\frac{\Delta x^*}{2}} + f^{(q)}_{\alpha-\frac{\Delta x^*}{2}}\right)\right]; \qquad (10)$$

$f_{(\alpha)}^{(h,q)}$ is thus seen to consist of an amplitude restoring operation at level h on the operator $F_{(\alpha)}^{(q)}$ which in turn consists of a two-point linear interpolation on the field of $f_j^{(q)}$ at the point α which is midway between the interim grid points $\alpha + \frac{\Delta x^*}{2}$ and $\alpha - \frac{\Delta x^*}{2}$. The $f_j^{(q)}$ consist of the original grid point values of the function (f_i, $f_{i\pm i}$, ...) as well as interpolated values obtained from previous applications of (10) with amplitude restoration at the level q. To the extent that the $f_j^{(q)}$ are homogeneous, there will be no phase error in the $f_{\alpha}^{(h,q)}$. Since the $f_j^{(q)}$ consist of both original and interpolated grid point values of f(x), they cannot be completely homogeneous, but the degree of homogeneity depends on the level of restoration (q) and is therefore to a large extent controllable. After final application of (10), with m = M, original grid point values of the function f(x), or interpolated values with corrected phase and amplitude, are available at all points $i + s/2^{M+1}$ where s = 1, 2, 3, ... , $(2^{M+1}-1)$.

The growth of the size of the stencil of operator (10) depends not only on h and q but also on m and p. Thus, when m = 0, (10) reduces to the amplitude restoring operator (9), and the number of data points involved in the stencil represented by

(10) is 2 (h + 1); when m = 1, and q = h the number is 2 + 3 h; but when m is equal to or greater than 2, the number of terms also depends upon p which determines the position of α between the points i and i + 1. For example, as can be seen from Table 1, when m = 2 and h = 1, there are 5 terms in the stencil for r = 1/8, but 6 terms for r = 3/8. On the other hand, for the same value of m, but with h = 3, there are 13 terms for the r = 1/8 position and only 12 terms for the r = 3/8 position.

Table 1. Coefficients of the Interpolation Stencils for Amplitude and Phase Restoration in Terms of the Original Grid Point Values for Various Values of m, r, and h (where q is taken equal to h)

A: m = 0; r = 1/2					
	h = 0	h = 1	h = 2	h = 3	h = 4
$Z_{i-4\Delta x}$					.00053406
$Z_{i-3\Delta x}$				-.00244140	-.00617981
$Z_{i-2\Delta x}$			.01171875	.02392578	.03460693
$Z_{i-\Delta x}$		-.0625	-.09765625	-.11962891	-.13458252
Z_i	.5	.5625	.58593750	.59814453	.60562134
$Z_{i+\Delta x}$	.5	.5625	.58593750	.59814453	.60562134
$Z_{i+2\Delta x}$		-.0625	-.09765625	-11962891	.13458252
$Z_{i+3\Delta x}$			.01171875	.02392578	.03460693
$Z_{i+4\Delta x}$				-.00244140	-.00617981
$Z_{i+5\ x}$					.00053406
B: m = 1; r = 1/4					
	h = 0	h = 1	h = 2	h = 3	h = 4
Z_{i-6}					-.00000330
Z_{i-5}				.00000596	-.00003368
Z_{i-4}				.00023365	.00094127
Z_{i-3}			-.00114441	-.00403047	-.00754994
Z_{i-2}		.00390625	.01640320	.02710342	.03564901
Z_{i-1}		-.07031250	-.10258484	-.12007284	-.13095344

Table 1. Coefficients of the Interpolation Stencils for Amplitude and Phase Restoration in Terms of the Original Grid Point Values for Various Values of m, r, and h (where q is taken equal to h) (Cont)

B: m = 1; r = 1/4 (Cont)					
	h = 0	h = 1	h = 2	h = 3	h = 4
Z_i	.75	.84375000	.87089539	.88179588	.88708519
Z_{i+1}	.25	.25781250	.26206970	.26671171	.27098010
Z_{i+2}		-.03515625	-.05149841	-.06254196	-.07102302
Z_{i+3}			.00572205	.01174092	.01745304
Z_{i+4}			.00013733	.00088787	-.00268873
Z_{i+5}				-.00005841	.00012805
Z_{i+6}					.00001518
Z_{i+7}					.00000029
C: m = 2; r = 1/8					
	h = 0	h = 1	h = 2	h = 3	h = 4
Z_{i-7}					-.00000002
Z_{i-6}				-.00000001	-.00000382
Z_{i-5}				.00000998	-.00002444
Z_{i-4}			-.00001341	.00019600	.00069724
Z_{i-3}			-.00109041	-.00303826	-.00520480
Z_{i-2}		.00439453	.01241863	.01854892	.02324251
Z_{i-1}		-.05175781	-.06990135	-.07875438	-.08409304
Z_i	.875	.94921875	.96389651	.96858347	.97055880
Z_{i+1}	.125	.11425781	.11541545	.11828768	.12100399
Z_{i+2}		-.01611328	-.02330482	-.02866947	-.03299573
Z_{i+3}			.00251234	.00523494	.00792706
Z_{i+4}			.00006706	-.00036325	-.00115760
Z_{i+5}				-.00003006	.00004125
Z_{i+6}				.00000014	.00000854
Z_{i+7}					.00000007
Z_{i+8}					+.00000000

Table 1. Coefficients of the Interpolation Stencils for Amplitude and Phase Restoration in Terms of the Original Grid Point Values for Various Values of m, r, and h (where q is taken equal to h) (Cont)

D: m = 2; r = 3/8					
	h = 0	h = 1	h = 2	h = 3	h = 4
Z_{i-7}					.00000001
Z_{i-6}					-.00000153
Z_{i-5}				.00000216	-.00002079
Z_{i-4}			.00000161	.00013145	.00081758
Z_{i-3}			-.00061691	-.00354297	-.00754953
Z_{i-2}		.00219727	.01531541	.02792382	.03854685
Z_{i-1}		-.07250977	-.10922849	-.13103966	-.14534869
Z_i	.625	.71240234	.74056983	.75361342	.76080201
Z_{i+1}	.375	.40869141	.42234743	.43101294	.43721260
Z_{i+2}		-.05053711	-.07718503	-.09466142	-.10721707
Z_{i+3}		-.00024414	.00860393	.01815371	.02687340
Z_{i+4}			.00019222	-.00153230	-.00441492
Z_{i+5}				-.00006058	.00028647
Z_{i+6}				-.00000057	.00001310
Z_{i+7}					.00000053
Z_{i+8}					-.0000000

As h increases, the number of terms in the stencils increases regardless of the value of m or p, but for $h \geq 3$ the additional terms are small in magnitude. Thus, it appears that as far as phase and amplitude errors are concerned, for all but the shortest wavelengths, there is little advantage in using orders of restoration higher than h = 3 or 4.

Figure 3 shows the phase error for the operator (10) as a function of level of restoration (H in the figure) and wavelength in units of the original grid length (Δx). The phase difference is shown for r = 0.25, for which the phase error is close to its maximum value for all wavelengths. For h = 0, the phase error is greater than 10^{-3} radians for waves up to about 15 to 16 grid lengths. For h = 1, the corresponding error occurs for waves 8 to 9 grid lengths. For h = 2, the threshold is

reached at waves of 6 to 7 grid lengths and for h = 3, the threshold is only about 5 grid lengths. But for h = 6, it decreases only slightly to 4 grid lengths. The amplitude error for (10) with q = h is essentially the same as that of the amplitude restoring operator (9) which is illustrated in Figure 1 for r = 0.5. Again, we see that, except for short waves, little further amplitude restoration takes place for h greater than 3 or 4.

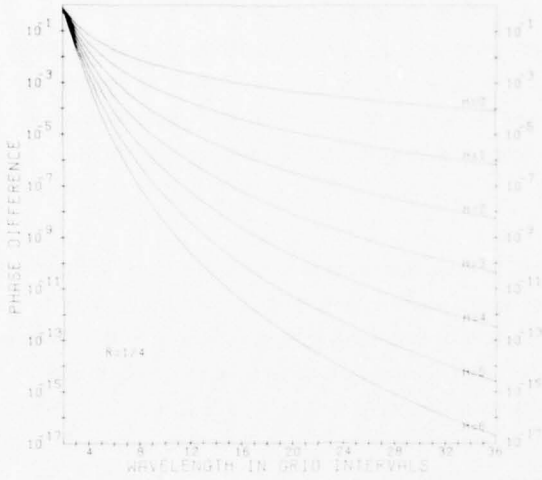

Figure 3. The Phase Error, in Radians for r = 0.25 for the Phase and Amplitude Restoring Interpolation Operator (10) as a Function of Level of Restoration H and Wavelength. The H = 0 curve corresponds to the 0.25 curve in Figure 2

For applications where some damping of the amplitude of the short waves is tolerable or desirable, there appears to be no advantage in exceeding levels of restoration corresponding to h = 3 or 4. It should be noted, in view of the fact that the magnitude of both the phase and amplitude error depends upon the position of the interpolation point α between the grid points i and i + 1, that one may wish to design an interpolation procedure in which the levels of restoration h and q are allowed to vary with position so as to compensate for this variation.

There is considerable flexibility in the manner in which operator (10) may be used, depending upon the nature of the application. The ability to correct for phase shift and amplitude truncation may find a wide variety of applications, but the application for which the present procedure is particularly appropriate is one which concerns the calculation of finite-differences involving both interpolated and original data points. The phase and amplitude errors produced by interpolation introduce an additional error in the finite differences. It may be beneficial to minimize such errors by the use of an appropriate high-order phase and amplitude restoring interpolation operator.

3. COMPARISON OF PHASE AND AMPLITUDE WITH PHASE RESTORING INTERPOLATION

While phase and amplitude restoring interpolation (10) is based upon the simpler amplitude restoring interpolation (9), it is at the same time more versatile and more limited in scope. Interpolation with (10) is defined only for those points $\alpha = 1 + r^*$ between the original grid points i and i + 1 such that r^* takes on the discrete values $S/2^{M+1}$ where S = 1, 2, 3, ... , $(2^{M+1} - 1)$. On the other hand, interpolation with (9) is defined for all points r between i and i + 1. Furthermore, in (9) as h increases, the size of the stencil increases uniformly and the amplitude response monotonically approaches unity for all wavelengths except the two-grid-interval wavelength. With (10), however, although phase is increasingly preserved as h and q increase for stencils of the same size, (9) is more efficient in amplitude preservation. Because of their differing characteristics direct comparisons were made between operators (9) and (10) in both a static and a dynamic framework.

3.1 Static Comparisons

In the static tests f(x) is represented in turn by a single periodic Fourier component varying from wave number 1 through wave number 35 in the interval 0 to 2π. Discrete values of f(x) are sampled at uniform subintervals $\Delta x = 2\pi/72$. These discrete values serve as data points from which interpolated values are obtained within each subinterval at specific values of r = 0.125, 0.25, 0.375, and 0.5. The root mean square error is then obtained for each wave number and for each value of r by comparing interpolated values with the functional values. The results are shown in Figures 4 through 8.

In these figures, the ordinate RMSE is the root mean square error for either the amplitude or phase and amplitude restoring interpolation, defined as,

$$\mathrm{RMSE} = \left\{ \frac{1}{72} \sum_{i=0}^{71} \left[f_{i+R} - \bar{f}_{i+R} \right]^2 \right\}^{1/2} ,$$

where f_{i+R} is the functional value of f(x) at the point i+R between i and i+1 and $\bar{f}_{i+R}$ is the corresponding interpolated value. The RMSE curves for amplitude restoring interpolation are indicated in the figures by RMSE followed by a single pair of parentheses. The number in the parentheses indicates the number of terms in the interpolation stencil. The curves for the phase and amplitude restoring interpolation are indicated by RMSE followed by two pairs of parentheses. The numbers in the first pair of parentheses indicate the order of the interpolation operator (h, q) and the number in the second pair of parentheses indicates the number of terms in the interpolation stencil. For each wave number f(x), and therefore f_{i+R}, is completely determined by the phase and amplitude of the wave. For each wave the amplitude was taken as 1 and the phase was taken as $-k\Delta x/2$ where k is wave number.

In Figure 4, with r = R = 0.5, M = 0 and therefore the amplitude restoring interpolation operator (9) is identical to the phase and amplitude restoring operator (10). The RMSE is shown for $f^{(0)}_{i+0.5}$ (the 2-point operator), through $f^{(4)}_{i+0.5}$ (the 10-point operator). For any wave number, RMSE monotonically decreases as the order of the operator increases. However, the decrease in RMSE is large and significant for the lower wave numbers and vanishingly small for the largest wave numbers. If one considers the spectral energy density distribution of most geophysical data, most of the variance is in the lower wave numbers and most of the noise is in the highest wave numbers. Therefore, for geophysical applications, the distribution of RMSE with wave number is highly advantageous, especially for the higher ordered operators.

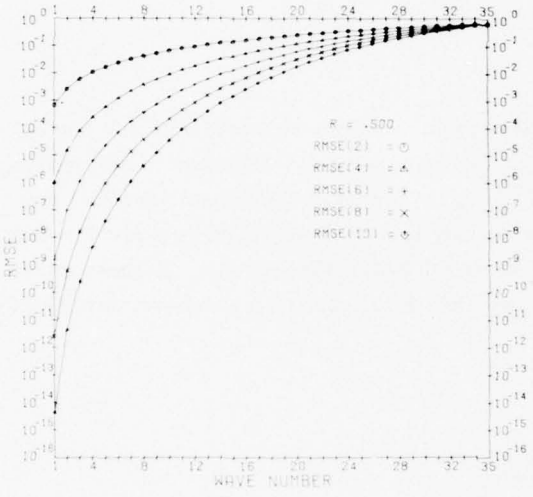

Figure 4. Root Mean Square Error (RMSE) for Amplitude Restoring Interpolation and Phase and Amplitude Restoring Interpolation for Various Wave Numbers in a 72-Grid-Interval Domain. The amplitude of each wave is 1.0 regardless of its wave number. Numbers in single parentheses indicate the size of the interpolation stencil. When the interpolation point R = 0.5, amplitude and phase and amplitude restoring interpolation are identical

In Figure 5, r = 0.125, there is a clear distinction between the amplitude restoring operators and the phase and amplitude restoring operators. The uppermost curve in the figure corresponds to $f^{(0)}_{i+0.125}$, the 2-point amplitude restoring operator. The next curve below this contains the superposition of $f^{(1)}_{i+0.125}$, $f^{(2)}_{i+0.125}$, $f^{(3)}_{i+0.125}$, and $f^{(4)}_{i+0.125}$. It is apparent that almost all of the improvement in RMSE that can be produced by amplitude restoration alone is effected by the 4-point operator, $f^{(1)}_{i+0.125}$. Further improvement in RMSE can be obtained by correcting for phase error at the same time that amplitude restoration is taking place, that is, by using operator (10) rather than operator (9). There is a steady decrease in the size of RMSE with the use of (10) as the order of the operator increases from

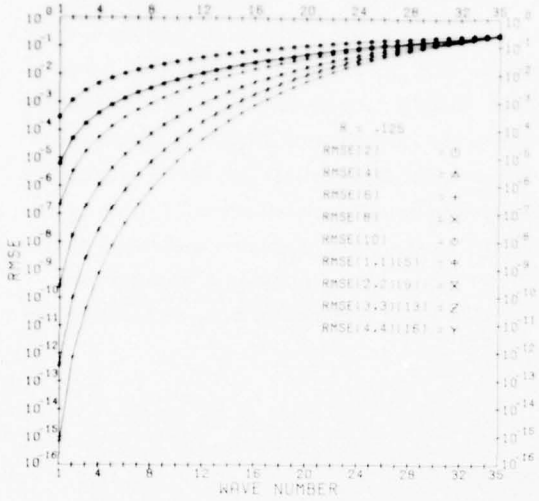

Figure 5. Same as Figure 4 with R = 0.125. The order (h, q) of phase and amplitude restoring interpolation is indicated by the numbers in the first pair of parentheses for those curves identified by two pairs of parentheses. The number in the second pair of parentheses indicates the size of the interpolation stencil

h = q = 1 through h = q = 4. In fact, the 5-point operator obtained with the use of (10), with h = q = 1, provides a RMSE distribution which is superior to that arising from the use of the 10-point operator $f^{(4)}_{i+0.125}$. Similar, though not identical results, are obtained at other values of r as can be seen from Figures 6 and 7 which show the RMSE distributions for r = 0.25 and 0.375, respectively. In these cases, RMSE (1, 1) is superior to RMSE (10) only for the lower wave numbers, but RMSE (2, 2) is clearly superior.

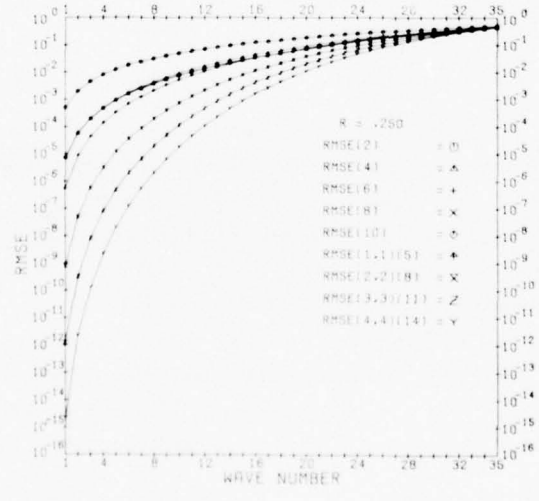

Figure 6. Same as Figure 5 with R = 0.25

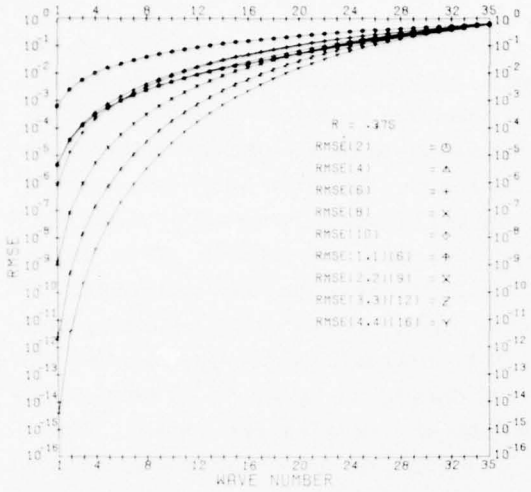

Figure 7. Same as Figure 5 with R = 0.375

In Figure 8, for r = 0.25, a sampling of results is shown for operator (10) with $h \neq q$. Although, in general, the results with $h \neq q$ are inferior to those with $h = q$, even where the stencil sizes are comparable, these results illustrate one of the versatile features of the phase and amplitude restoring interpolation; namely, the size of the stencil can be tailored to fit changing circumstances.

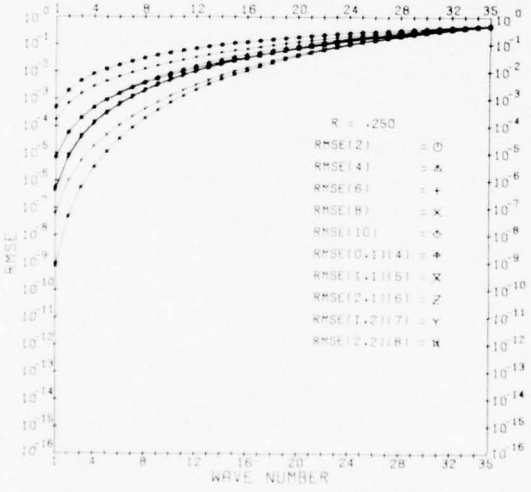

Figure 8. Same as Figure 5 with R = 0.25

3.2 Dynamic Comparisons

Dynamic tests were carried out in a simple system that approximates the complexity of operational, multilevel, primitive equation models. The eight-level primitive-equation channel model is fully described in an earlier study.[35] It was used to compare amplitude restoring interpolation to two-point linear interpolation, with results which are outlined in the Introduction. The same basic framework is used in the present study with some differences in detail, necessitated primarily in order to accommodate tests with phase and amplitude interpolation. Thus, in the present study, the fine-mesh grid size is 1/4 the size of the coarse-mesh grid (555/4 km) rather than 1/5 as in the earlier study. The amplitude restoring interpolation in the present study makes use of the more efficient inverse operator (6) rather than the multiplicative operator described by the author.[36] In addition, the smoothing operators used in the present study are not only more efficient,[39] but are applied in a slightly different fashion. Finally, in order to permit an unbiased basis for judging the merits of each test solution, a fine mesh validation (FMV) solution was obtained.

All test solutions, including FMV, start with the same smooth coarse-mesh solution at time step 6000 (83.33 days) as initial data. IN FMV, the coarse-mesh initial fields of velocity and temperature were interpolated throughout the entire coarse-mesh domain using the high-order phase and amplitude restoring interpolation operator (10), with $h = q = 3$ wherever possible, and reducing the order of the operator only in approaching the northern or southern boundary. FMV solutions were obtained throughout the entire domain with the fine-mesh solution in space (138.75 km) and time (5 min), for 1600 time steps. These solutions then serve as validation solutions for the fine-mesh nested solutions since they are obtained without any artificial internal boundaries and except for the initial interpolation at 83.33 days, without any further interpolation.

Three separate series of test solutions in the nested fine-mesh domain were carried out from the same coarse-mesh initial conditions and with precisely the same conditions in all respects except for the type of interpolation used to obtain the initial information and continuing boundary information.

Series A, amplitude restoration, makes use of Eq. (9) with $h = 3$. Series B, phase and amplitude restoration, makes use of Eq. (10), with $h = q = 3$ at all points where it is possible to do so. Since the northern boundary of the fine-mesh domain is situated at 17.5 deg N, there are only three coarse-mesh grid points north of this boundary. After the initialization for the fine-mesh experiments interpolation is performed only one dimensionally from the continuing coarse-mesh solutions onto the fine-mesh boundaries. Since the coarse mesh domain is periodic in the east-west direction, there is no difficulty in using Eq. (10), with $h = q = 3$ on the

northern and southern fine-mesh boundaries. However, it is necessary to gradually decrease the order of interpolation on the eastern and western boundaries for some of the grid points near the northern boundary.

The grid spacing is uniform in the east-west (x) and north-south directions and is 555 km in the coarse-mesh and 138.75 km in the fine-mesh configuration. The vertical spacing is 125 mb in both mesh systems. The northern and southern boundaries are located at 32.5 deg N and 32.5 deg S in the large-scale model, and at 17.5 deg N and 2.5 deg N in the fine-mesh model (see Figure 9). The east-west domain extends over 20 grid intervals (11,100 km) and is periodic in the coarse-mesh domain. In the fine-mesh nested region the east-west domain contains 16 grid intervals (2220 km) and is not periodic. The north-south domain contains 13 grid intervals in the coarse-mesh region (7215 km) and 12 grid intervals (1665 km) in the fine-mesh nested region. Thus, if i and j represent east-to-west and south-to-north grid point index designations, i varies from 1 through 17 and j, from 1 through 13 in the fine-mesh nested region. Thus, at j = 8, north-south interpolation on the eastern and western boundaries makes use of a lower-order form of Eq. (10) with h = 2 and q = 3. At j = 9, on the eastern and western fine-mesh boundaries there is no need for interpolation since these points correspond to coarse-mesh points. This is also true at j = 13. At j = 10 we use Eq. (10) with h = 3 and q = 2 and at j = 12, with h = q = 2. At j = 11, the interpolation point α lies midway between the coarse-mesh points and so Eq. (10), with h = q = 3, reduced to Eq. (9), with h = 3.

In the Series C tests, only two-point linear interpolation is used.

To recapitulate, the following procedure was followed in the various tests.

(1) Starting from a stationary motion field, with no horizontal temperature differences and a vertical temperature distribution appropriate for the tropics, the heating function is turned on in the large-scale domain and motion begins to develop.

(2) The coarse-mesh run is continued beyond 6400 time steps of 20-min duration for a total elapsed time of about 90 days.

(3) Starting at time step 3000 we performed occasional smoothing with a high-order, amplitude restoring operator[39] on the predicted fields of horizontal velocity and temperature. The 9-point smoothing operator, shown in Table 2 with p = 3, was used in both the east-west and north-south directions whenever it was possible to do so. For those points situated four grid points or less from the northern or southern boundary 7-, 5-, and 3-point operators were used as appropriate in both the east-west and north-south directions. These operators are also shown in Table 2 with p = 2, 1, or 0, respectively. Thus, although the smoothing was performed only occasionally, the boundary regions of the domain were more strongly smoothed inasmuch as lower-order operators were used near the boundaries. The smoothing was performed only every 1000 time steps between time steps 3000 and 5000, but then the frequency of smoothing was increased to every 10 time steps from step 5010 through step 6000. This produced smoothed fields for the initial times for the various test runs.

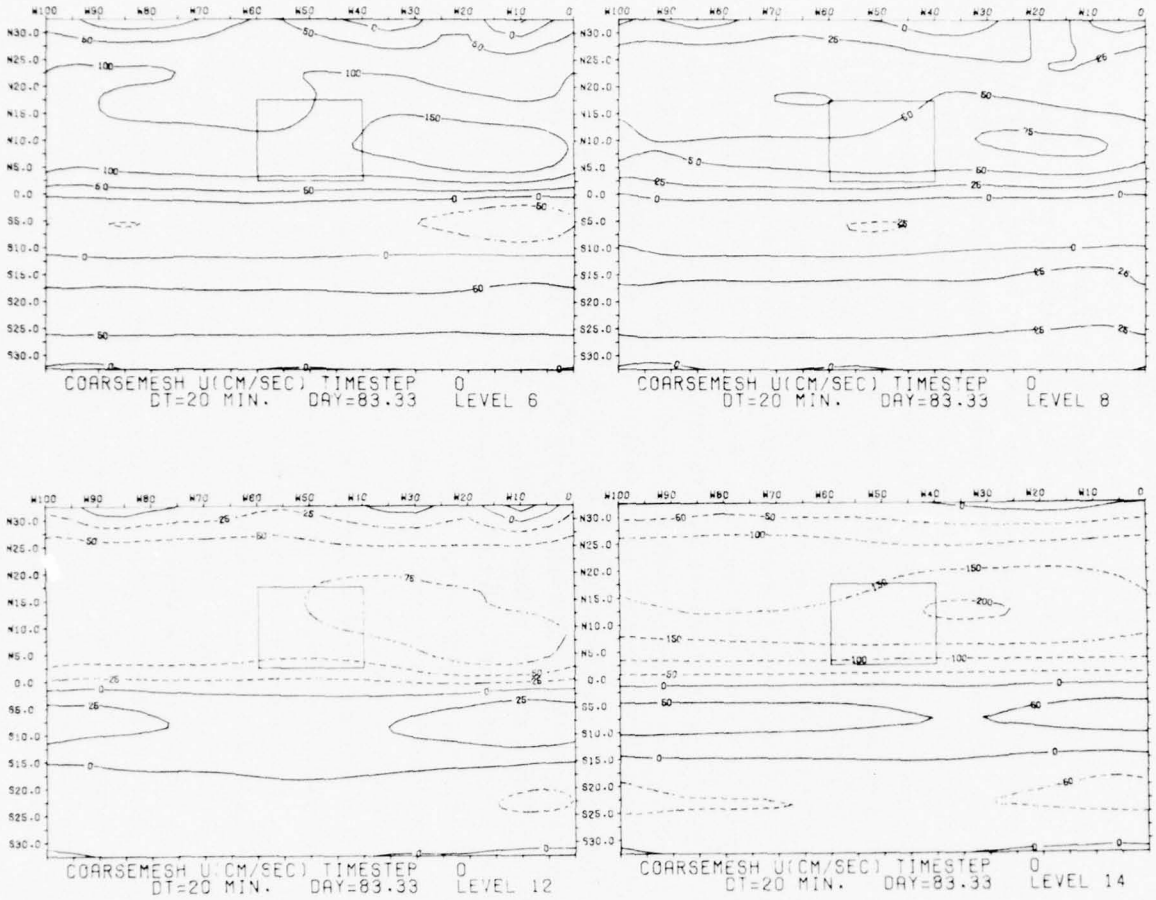

Figure 9. The Distribution of Zonal Wind Velocity (cm sec^{-1}) on Day 83.33 in the Large-Scale, Coarse-Mesh Domain for Two Upper Levels (level 6, 312.5 mb; level 8, 437.5 mb) and Two Lower Levels (level 12, 687.5 mb; level 14, 812.5 mb). Solid curves indicate flow from west to east; dashed curves from east to west. The rectangular inset indicates the size and location of the fine-mesh, nested domain

Table 2. Stencils for $f_i^{(p+1)}$ for Various Values of p

p		f_i	$f_{i\pm 1}$	$f_{i\pm 2}$	$f_{i\pm 3}$	$f_{i\pm 4}$	$f_{i\pm 5}$	$f_{i\pm 6}$	$f_{i\pm 7}$	$f_{i\pm 8}$	$f_{i\pm 9}$	$f_{i\pm 10}$
0	$1/2^2$	(2	1)									
1	$1/2^4$	(10	4	-1)								
2	$1/2^6$	(44	15	-6	1)							
3	$1/2^8$	(186	56	-28	8	-1)						
4	$1/2^{10}$	(772	210	-120	45	-10	1)					
5	$1/2^{12}$	(3172	792	-495	220	-66	12	-1)				
6	$1/2^{14}$	(12952	3003	-2002	1001	-364	91	-14	1)			
7	$1/2^{16}$	(52666	11440	-8008	4368	-1820	560	-120	16	-1)		
8	$1/2^{18}$	(213524	43758	-31824	18564	-8568	3060	-816	153	-18	1)	
9	$1/2^{20}$	(863820	167960	-125970	77520	-38760	15504	-4845	1140	-190	20)	-1)

(4) For the principal series of experiments, starting from day 83.33, both the coarse-mesh solutions (which were used to supply boundary information for the nested, fine-mesh solutions) and the various fine-mesh solutions (including FMV) were smoothed at 2000-min intervals (every 100 coarse-mesh time steps or every 400 fine-mesh time steps). This is a departure from the earlier study[35] in which the smoothing interval was only 200 min. However, other tests in the present study were carried out with more frequent smoothing; namely, at intervals of 250 min and 50 min in order to separate the effects of smoothing from those of interpolation.

The results of the various test solutions and comparisons with the FMV solutions are shown for two separate times; namely, at 800 fine-mesh time steps (day 86.11) and at fine-mesh time step 1600 (day 88.89). As in the earlier study,[35] the east-west component of the velocity (u) is used to illustrate the relative merits of the various test runs. The results are shown both graphically in several figures and in Tables 3 and 4, which show the correlations between FMV and the various test solutions as well as the root mean square differences between them.

Table 3. Root Mean Square Differences (RMSD) of the Zonal Wind Field in cm sec^{-1} Between Fine Mesh Validation Smoothed Every 2000 min (FMV 2000) and Other Model Solutions After 800, 5-min Time Steps (day 86.11) and 1600 Time Steps (day 88.89). Results apply only to the limited-area domain

Level	Day 86.11									
	AS2000	BS2000	CS2000	AS250	BS250	CS250	AS50	BS50	CS50	FMV250
2	25.3	24.4	31.7	9.4	9.3	12.8	5.5	5.5	9.2	0.3
4	12.8	12.4	13.6	8.9	8.9	10.3	8.5	8.5	10.2	0.4
6	7.1	6.8	7.1	5.5	5.5	6.0	5.8	5.8	6.6	1.0
8	4.3	4.1	4.2	2.7	2.7	3.0	2.5	2.6	3.1	0.5
10	4.7	4.7	4.6	4.1	4.1	3.9	3.9	3.9	3.8	1.0
12	4.1	4.1	3.9	3.2	3.3	2.9	3.0	3.0	2.9	0.4
14	7.9	7.6	8.8	4.8	4.8	6.2	5.9	5.9	7.5	0.4
16	5.6	5.5	6.0	4.3	4.3	4.8	4.8	4.8	5.6	0.3
	Day 88.89									
2	36.9	35.8	41.8	13.1	12.9	14.6	7.7	7.7	10.1	0.7
4	16.0	15.6	16.1	10.6	10.5	11.8	10.3	10.3	11.8	0.6
6	15.8	15.4	15.1	13.3	13.2	13.1	12.8	12.7	12.8	2.0
8	6.6	6.5	6.5	5.6	5.7	5.5	5.0	5.0	5.4	1.3
10	10.7	10.7	10.5	10.0	9.9	9.8	10.0	10.0	10.0	1.5
12	8.1	8.0	8.9	7.1	7.1	6.8	6.9	6.8	6.8	0.9
14	9.6	9.5	10.9	6.5	6.5	6.7	7.0	6.9	7.6	0.7
16	6.7	6.6	7.6	3.8	3.8	4.4	4.3	4.3	5.1	0.5

Figure 10 shows the distribution of zonal velocity in FMV at day 86.11 for two upper levels (level 6, 312.5 mb; level 8, 437.5 mb) and two lower levels (level 12, 687.5 mb; level 14, 812.5 mb), but only for the area occupied by the nested region. Figures 11 through 13 show the comparable results for Series A, B, and C. Flows from west to east are indicated by solid lines and flows from east to west by dashed lines. In Figures 10 through 13, smoothing is performed every 400 time steps, that is, only twice from the initial time (day 83.33) until day 86.11. In spite of the insignificant amount of smoothing the FMV results, for the nested region, are smooth at all levels. However, the results shown for Series A, B, and C are not as consistently smooth. There is little difference among the three series at the two upper levels, and each shows quite good agreement with FMV, at least as far as the larger scale features are concerned. The minor differences that are apparent among the three series are in the direction, not unexpectedly, of increasing smoothness and versimilitude (with regard to FMV) in proceeding from Series C

Table 4. Linear Correlation Coefficients Between the FMV 2000 Zonal Wind Field and the Zonal Wind Fields for Other Model Solutions Calculated for the Limited-Area Domain

Level	Day 86.11									
	AS2000	BS2000	CS2000	AS250	BS250	CS250	AS50	BS50	CS50	FMV250
2	.991	.992	.986	.999	.999	.999	1.000	1.000	1.000	1.000
4	.990	.992	.990	.998	.998	.999	.998	.998	.999	1.000
6	.944	.949	.937	.969	.969	.957	.959	.959	.945	.999
8	.946	.951	.947	.981	.982	.979	.986	.985	.980	.999
10	.889	.891	.885	.912	.909	.929	.928	.929	.938	.995
12	.952	.951	.954	.970	.968	.975	.976	.975	.978	.999
14	.983	.984	.979	.994	.994	.994	.995	.995	.995	1.000
16	.974	.975	.974	.984	.984	.987	.986	.985	.988	1.000
	Day 88.89									
2	.978	.979	.970	.998	.998	.998	.999	.999	.999	1.000
4	.982	.984	.983	.996	.996	.997	.996	.996	.996	1.000
6	.685	.702	.704	.771	.772	.773	.783	.785	.780	.995
8	.866	.869	.874	.919	.915	.928	.933	.932	.927	.996
10	.557	.554	.574	.631	.631	.647	.623	.621	.632	.994
12	.810	.817	.773	.869	.869	.868	.866	.866	.865	.998
14	.968	.969	.961	.984	.983	.987	.984	.985	.987	1.000
16	.965	.966	.958	.988	.988	.991	.989	.989	.991	1.000

to Series A to Series B. At the lower levels, however, there are sizable and evident boundary effects in the C series (two-point interpolation), but relatively minor boundary effects in the A and B series. On the other hand, the results from the A and B series are virtually identical. In spite of the obvious boundary effects in Series C at the lower levels, the larger scale features of all three series closely resemble the FMV results.

The above conclusion is also evident from Tables 3 and 4 showing the root mean square differences (RMSD) and linear correlation coefficients, level for level, between FMV and each of the three series. In Tables 3 and 4, the series of solutions (A, B, C) as well as the time intervals between smoothing are indicated by the column headings. Thus, AS2000 indicates Series A with smoothing every 2000 minutes.

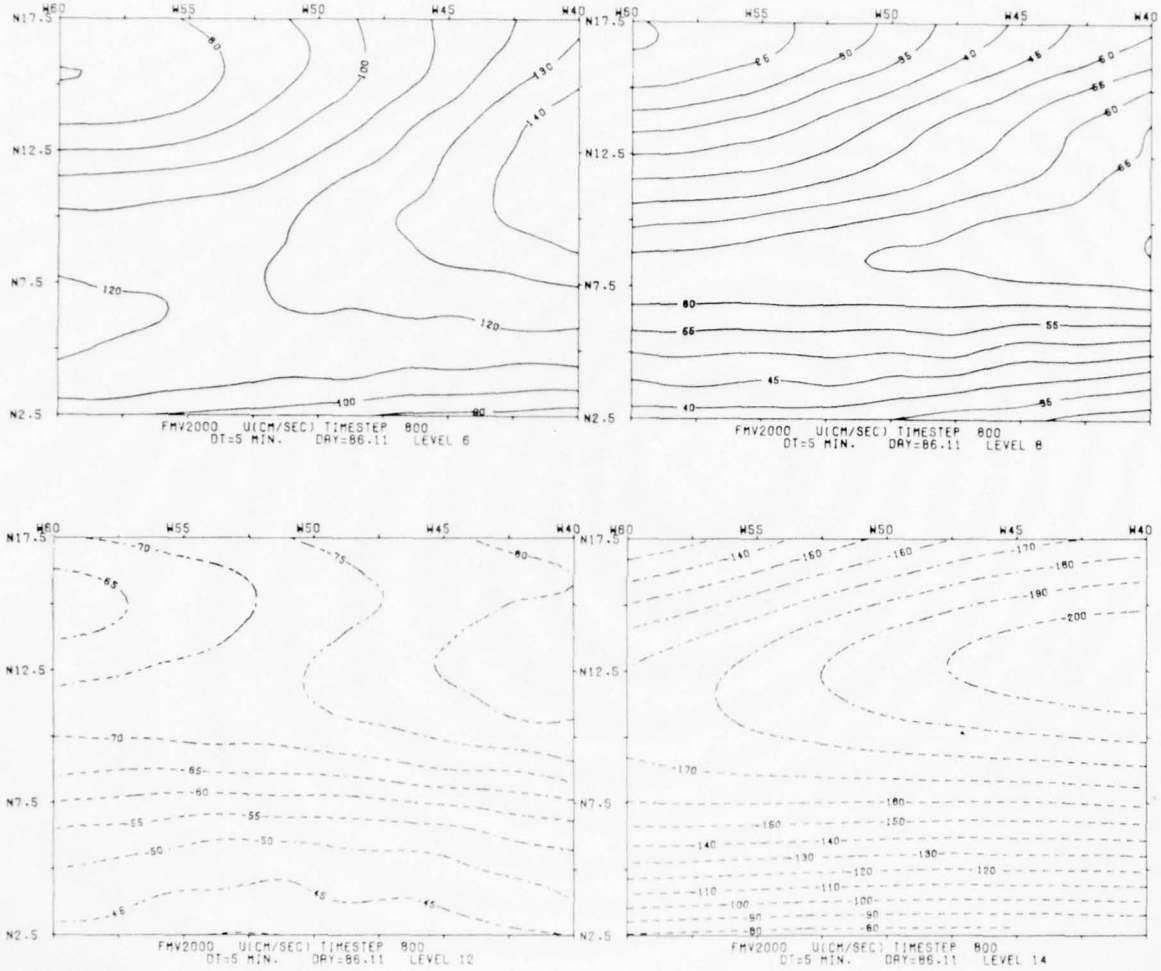

Figure 10. The Zonal Velocity Distribution for Levels 6, 8, 12, and 14 for the Fine Mesh Validation (FMV) Solution After 800, 5-min Time Steps (day 86.11). Although FMV solutions were obtained for the entire large-scale domain, only the results for the nested region are shown here. The frequency of smoothing is every 2000 min as indicated in the legend

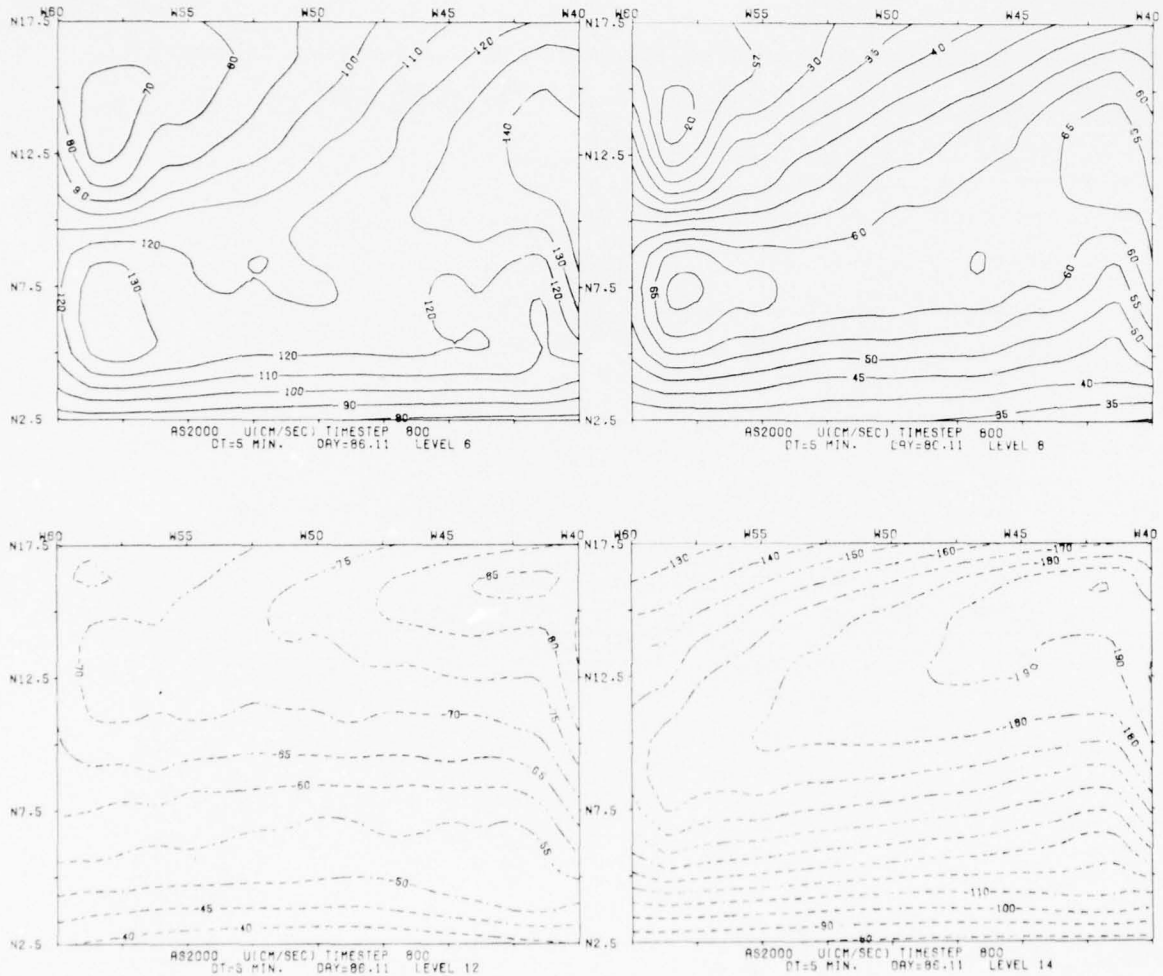

Figure 11. Same as Figure 10 for Series A, Amplitude Restoring Interpolation

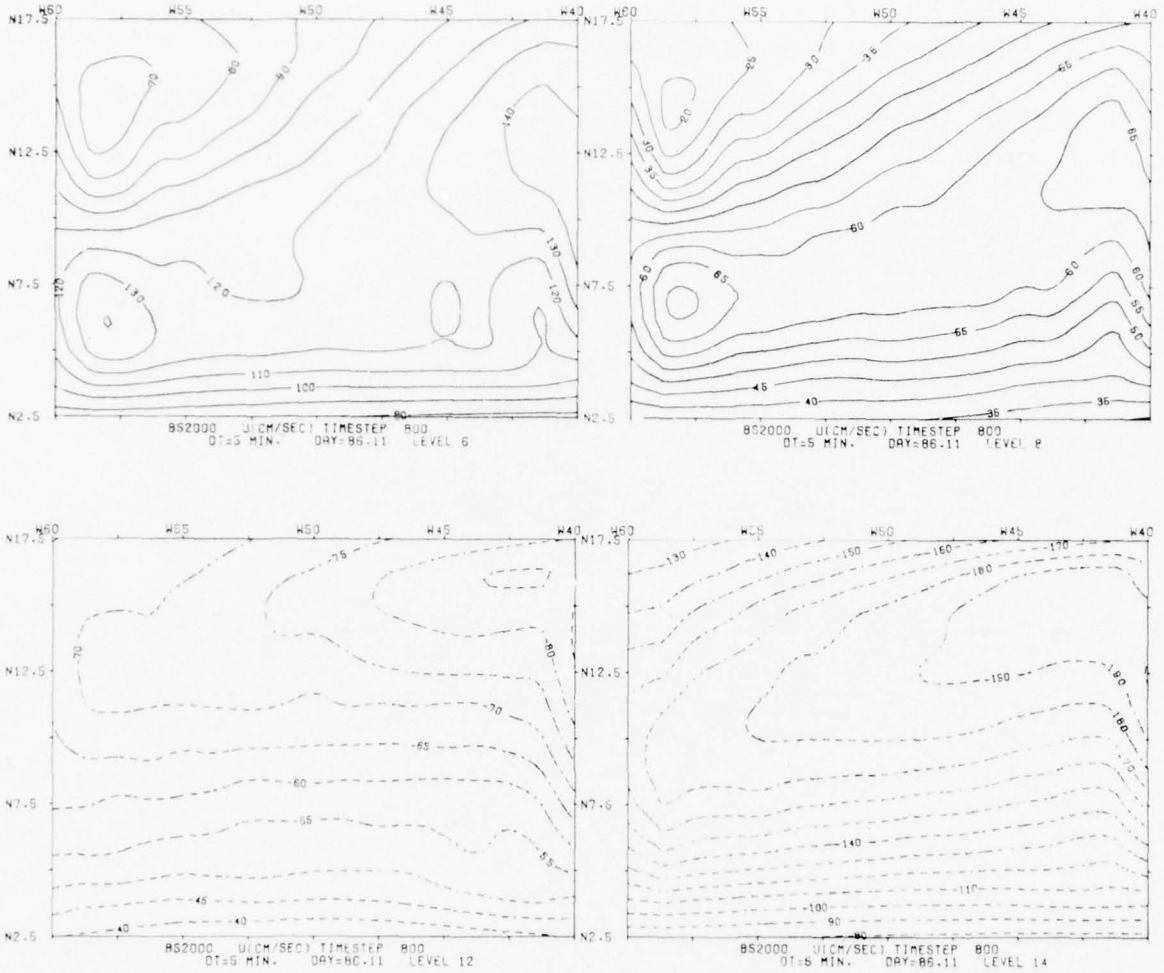

Figure 12. Same as Figure 10 for Series B, Phase and Amplitude Restoring Interpolation

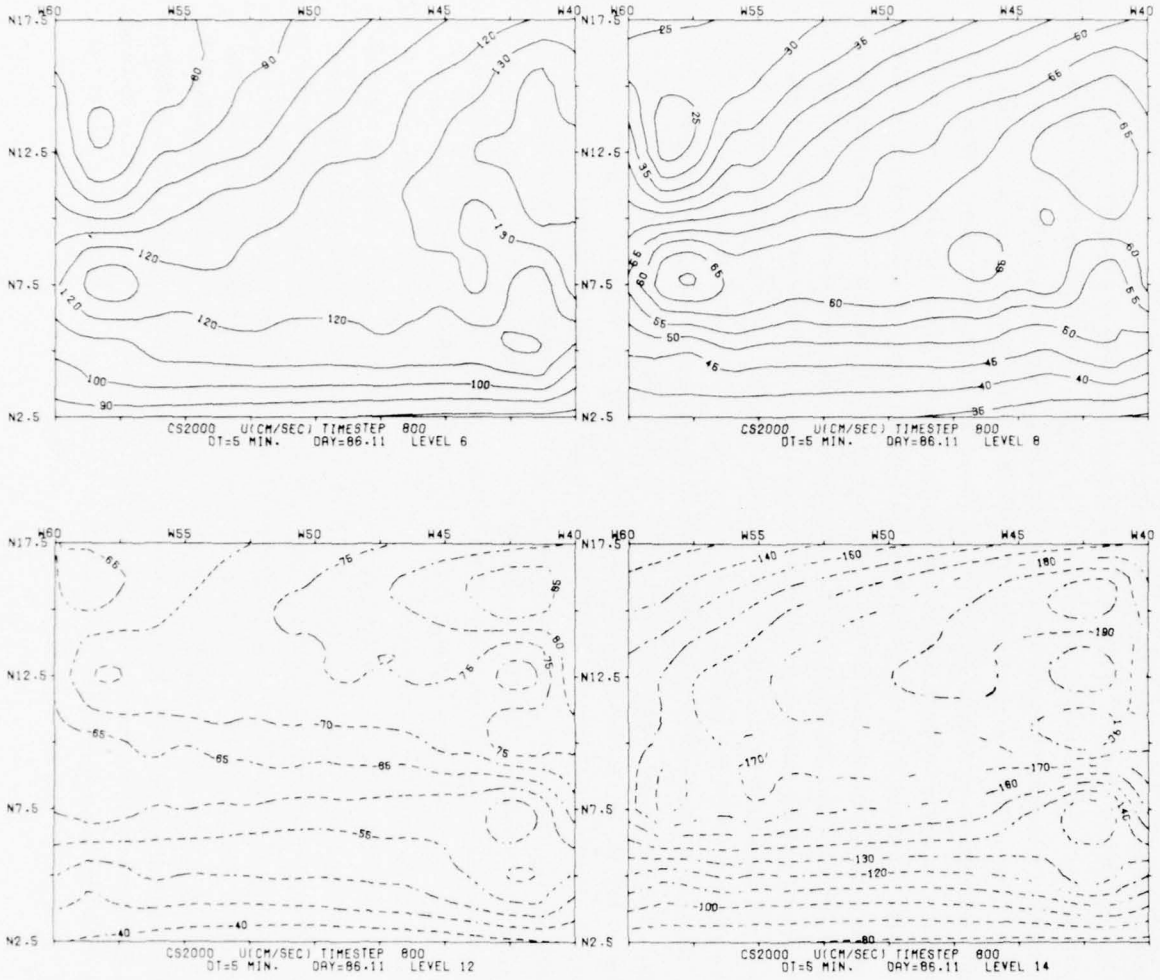

Figure 13. Same as Figure 10 for Series C, Two-Point Linear Interpolation

It is apparent that there is little difference among the solutions AS2000, BS2000, and CS2000 both with regard to the root mean square differences as well as with regard to the correlation coefficients. It is also apparent, as far as the RMSD's and correlation coefficients are concerned, that it is the large-scale features that contain most of the variance and therefore dominate the results.

In the earlier study,[35] where 1/5 mesh size was used in experiments comparable to Series A and Series C, there were far more pronounced boundary effects especially where two-point interpolation was used. The more evident boundary effects occurred in the earlier study in spite of much more frequent smoothing (every 200 min as compared with every 2000 min in the present study). This result points up the prominent role played by phase error in the boundary information since with 1/5 mesh size there is appreciable phase error at all interpolated points, whereas with 1/4 mesh size there is no phase error at the central interpolated point even in Series A and Series C. Nevertheless, it is apparent from Figure 12 that correcting for both phase and amplitude error in the interpolated boundary information is not sufficient by itself to avoid boundary effects. This conclusion is even more apparent from the results of the solution after 1600 time steps (day 88.89).

Figures 14 through 17 are comparable to Figures 10 through 13 but illustrate the results for day 88.89. The Series A and B results are somewhat "noisier" than they were on day 86.11, particularly at the upper two levels. Series C, Figure 17, however, is significantly noisier, at all levels on day 88.89 as compared with the results on day 86.11. However, in all three series the large-scale distribution has not changed appreciably. The FMV results on day 88.89 remain smooth, but show a new smaller-scale variation in the north-south direction which was not evident on day 86.11. None of the three test series (A, B, or C) show any evidence of this smaller-scale variation, although the larger-scale features of each continue to resemble the larger-scale features of FMV on day 88.89. This continued resemblance of the larger-scale features is reflected in Tables 3 and 4 by the still relatively small RMSD's and relatively large correlations between each of the series and FMV on day 88.89. There is some growth of RMSD and some small decrease in correlation between days 86.11 and 88.89, especially at the mid-levels where the flow changes from predominantly easterly to predominantly westerly. However, in spite of the growth of noise in the three test series, it is apparent that the RMSD's and correlations are dominated by the variance contained in the large-scale features. I shall return subsequently to the question of the smaller-scale features in FMV on day 88.89 which are not captured by any of the test series.

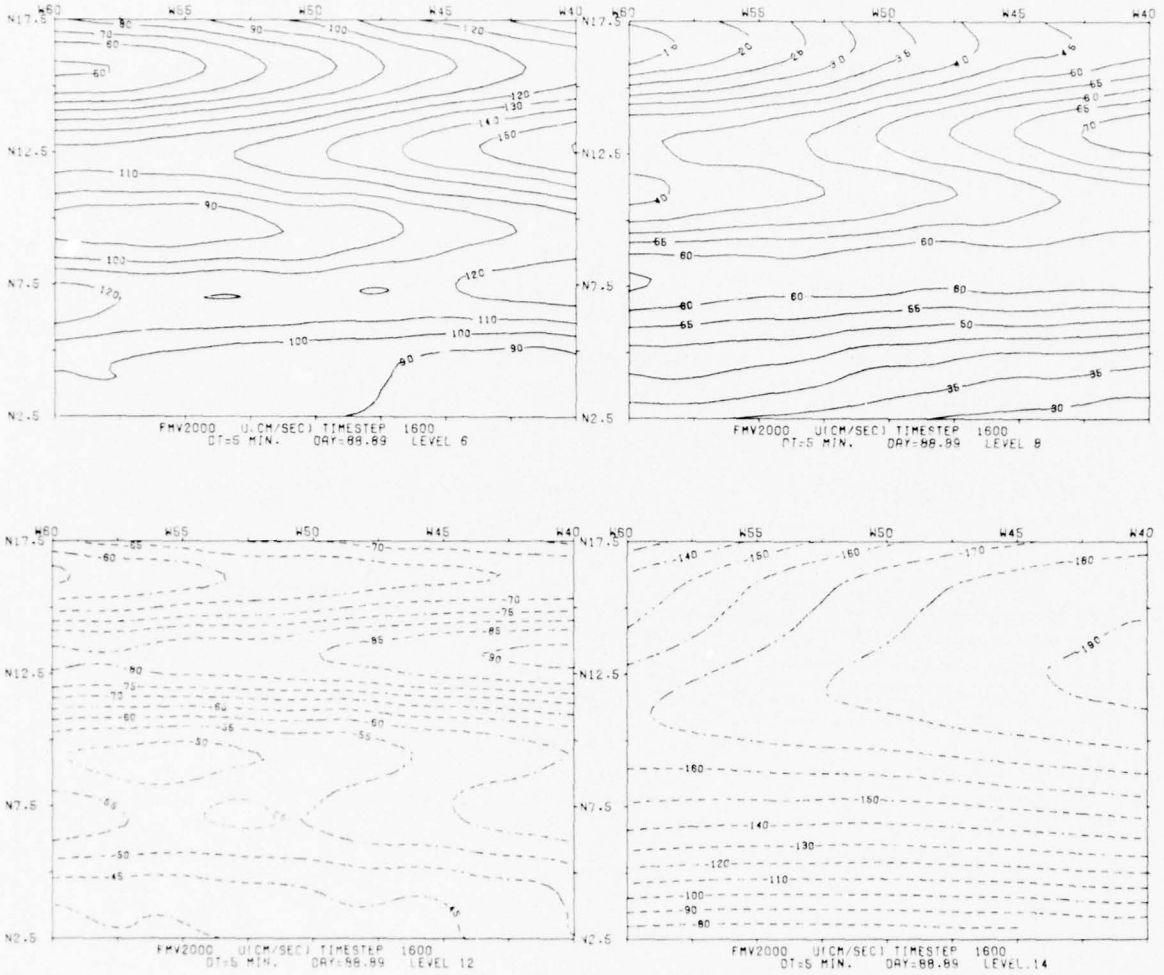

Figure 14. Same as Figure 10 for Day 88.89

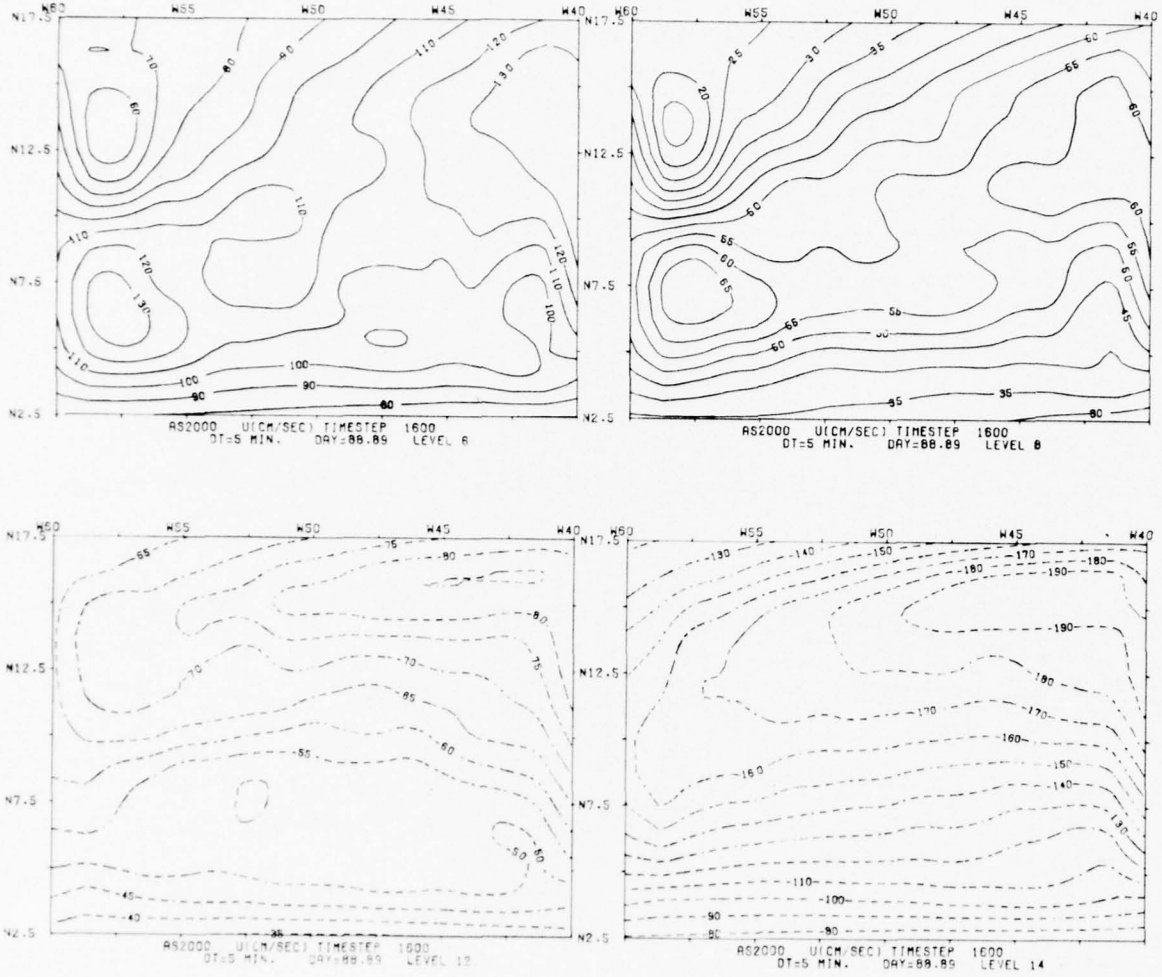

Figure 15. Same as Figure 11 for Day 88.89

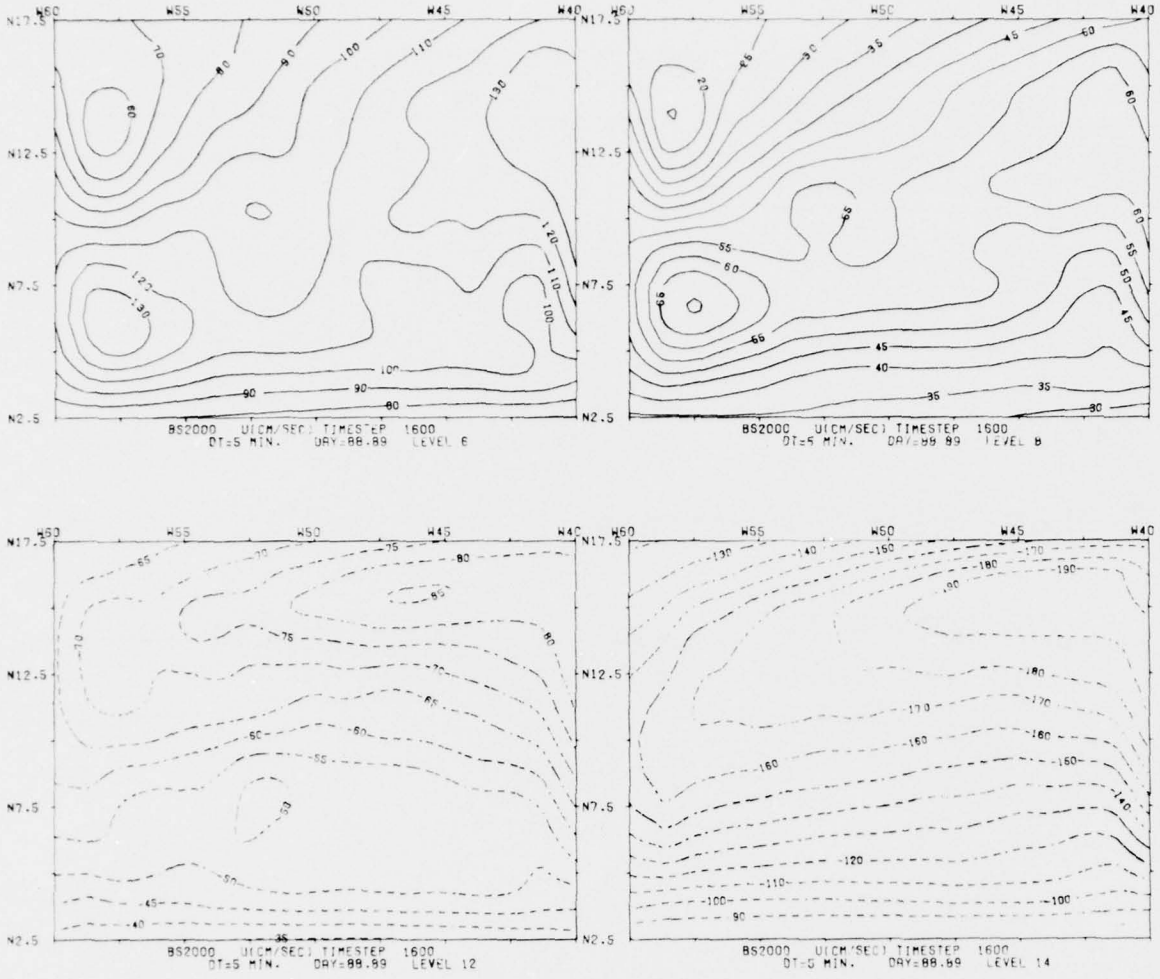

Figure 16. Same as Figure 12 for Day 88.89

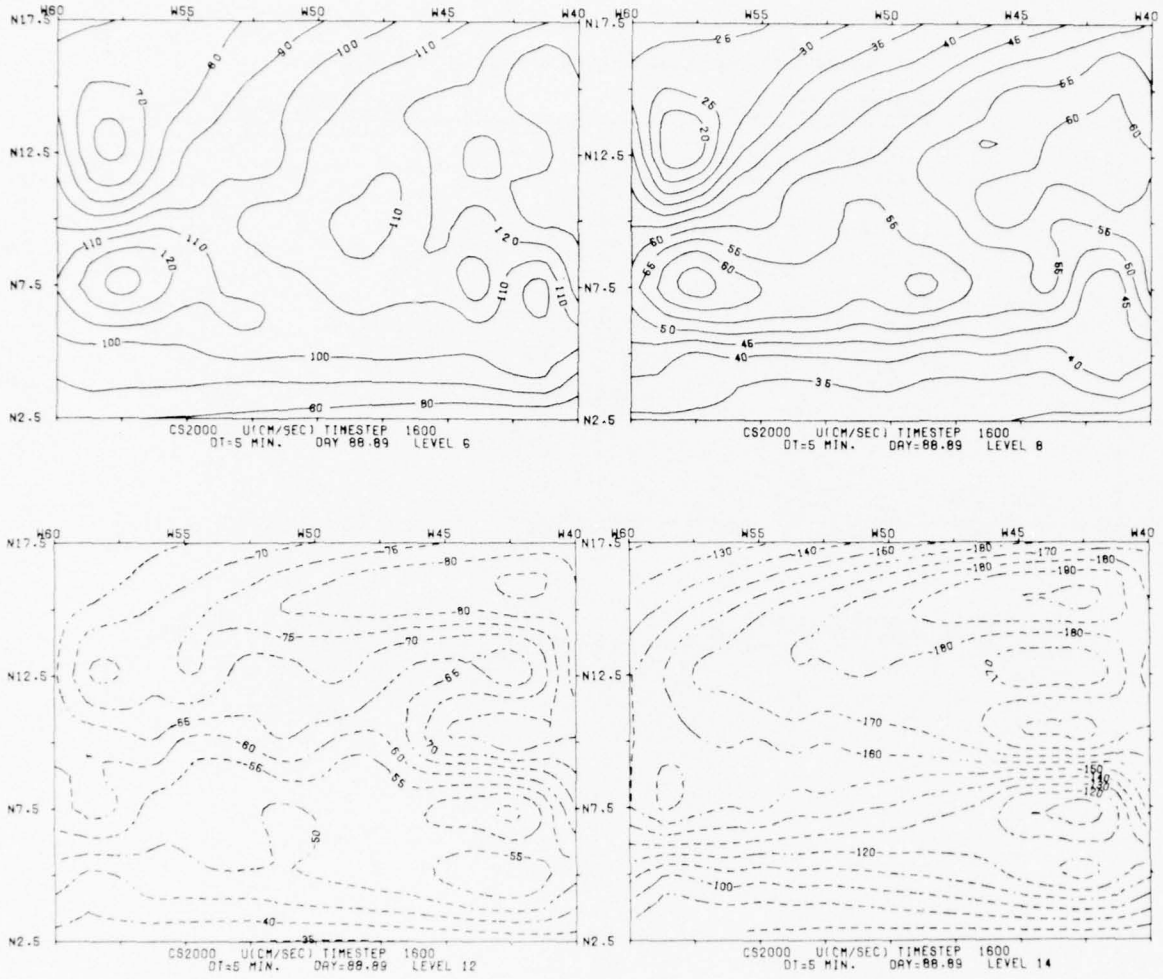

Figure 17. Same as Figure 13 for Day 88.89

It is apparent from the results that minimizing phase error in the boundary information used to obtain the limited area solutions is an important aspect in maintaining reasonable agreement between the test solution and the validation solution. However, it is also apparent, as has been mentioned, that there is an increasing growth of boundary generated noise as the solutions are carried forward in time, particularly in the Series C solutions. In the earlier study, with fine-mesh spacing 1/5 the coarse-mesh spacing, smoothing of the fields was carried out much more frequently (every 200 min) and yet, the results were affected to an even greater extent by boundary generated noise. In order to determine whether more frequent smoothing of the present solutions would be effective in decreasing this noise, two additional sets of solutions were obtained with the Series A, B, and C conditions. In each case the new Series A, B, and C solutions were obtained in precisely the same manner as the original series except for the frequency of smoothing. In one set the smoothing was performed every 250 min and in the other, every 50 min. The RMSD's and correlations between these sets of solutions and the original FMV solution are tabulated in Tables 3 and 4, under columns labeled S250 or S50. The zonal wind fields at levels 6, 8, 12, and 14 are shown for the AS250, BS250, and CS250 for day 86.11 (Figures 18 through 20) and day 88.89 (Figures 21 through 23). Figures 24 through 26 and Figures 27 through 29 show the comparable results for Series A, B, and C with smoothing every 50 min (that is, every ten time steps).

It is immediately apparent from the figures that the additional smoothing, even at intervals of 250 min, is sufficient to smooth out the minor boundary induced irregularities in all three series at the two upper levels. Furthermore, the major irregularities in the C series are also smoothed out at the two lower levels. In addition, the increased frequency of smoothing has the effect of substantially reducing the RMSD's and increasing the linear correlation between all three series and FMV. Compared with the earlier study in which smoothing was performed every 200 min, the improvement in all three series, with smoothing every 250 min, in reducing boundary induced irregularities, decreasing the size of RMSD's and increasing the correlation between the series and FMV is indeed remarkable and again focuses attention on the important difference between a 1/5 mesh size and the 1/4 mesh size of the present study. The difference between the former 1/5 and the present 1/4 mesh sizes is the only important difference between the earlier and the present studies as far as Series AS250 and CS250 (amplitude restoring and two-point interpolation) are concerned.

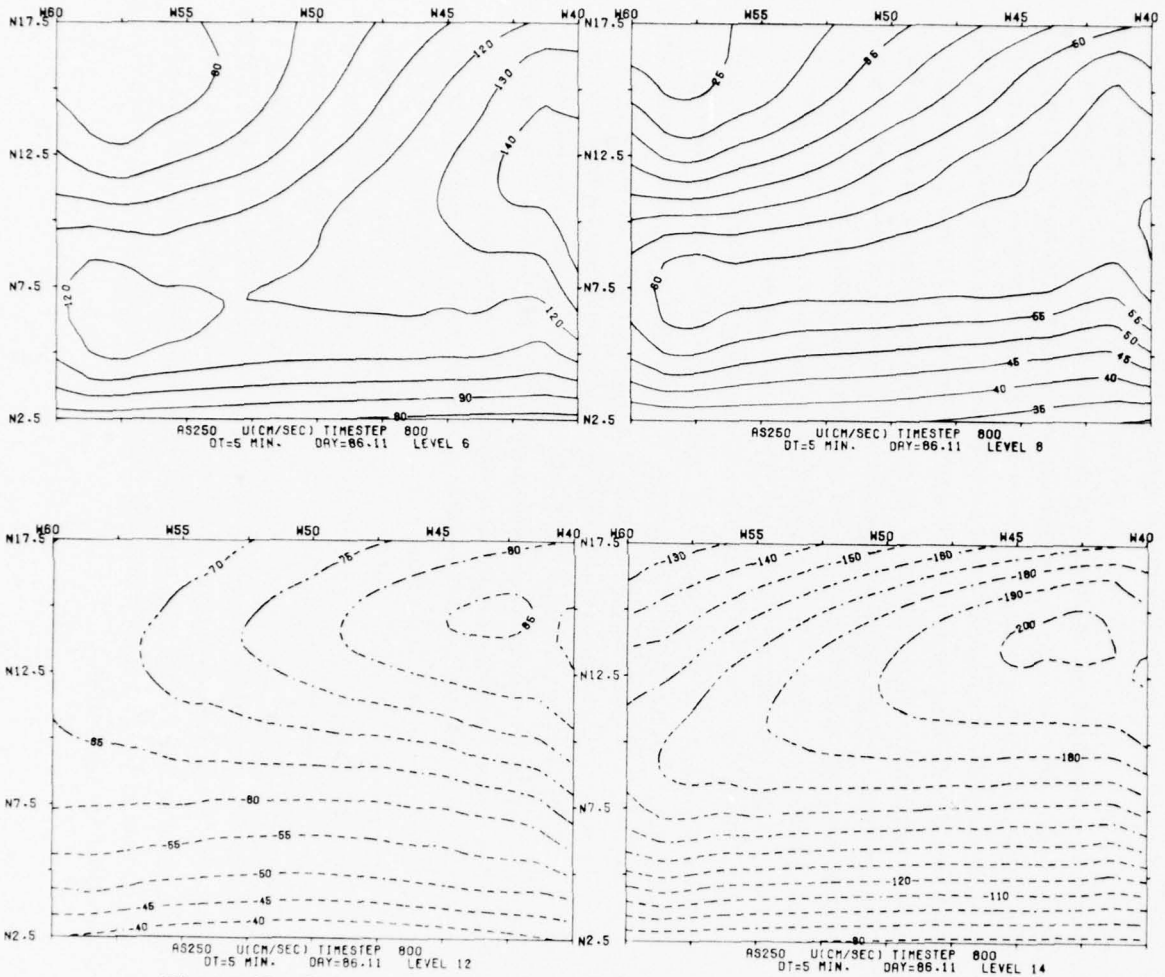

Figure 18. Same as Figure 11 with Smoothing Every 250 min (50 time steps)

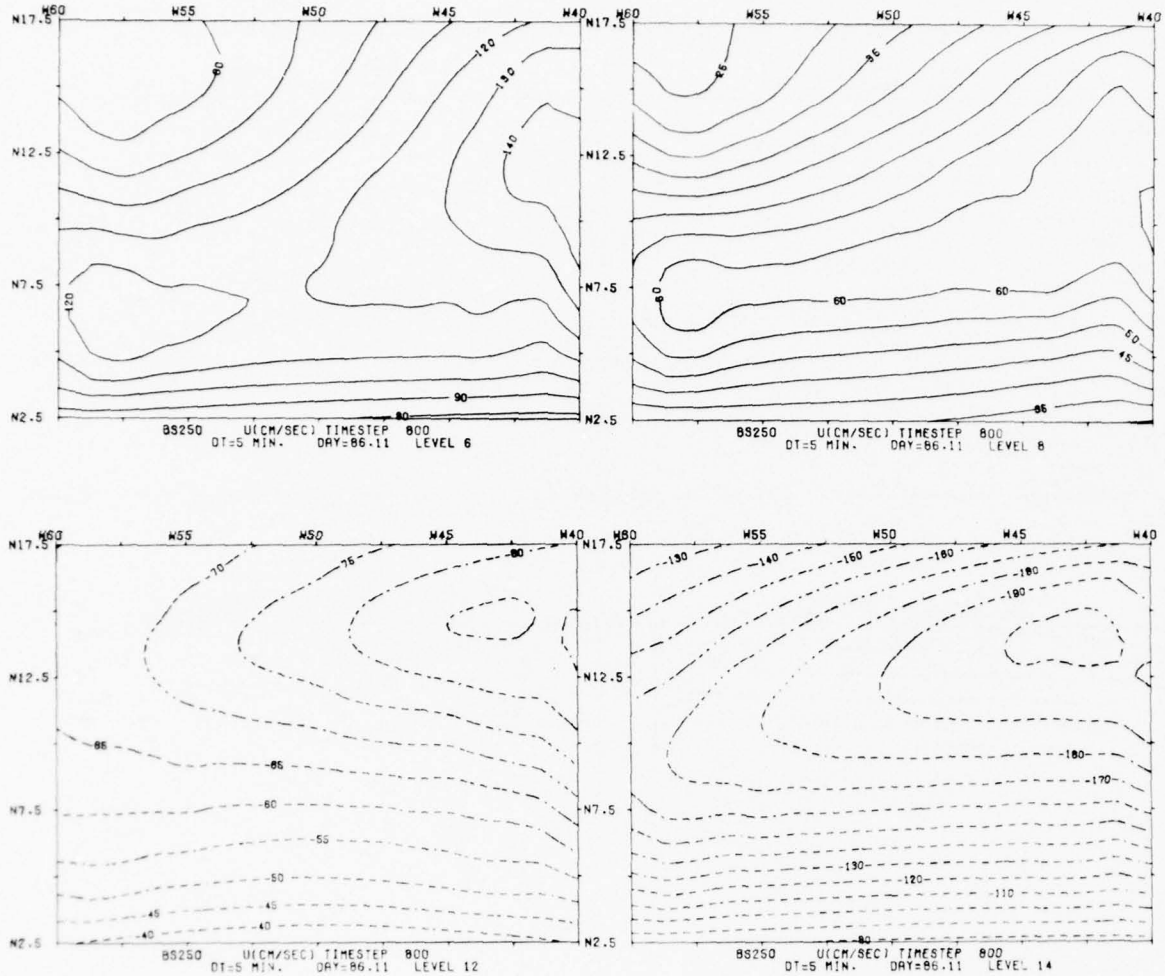

Figure 19. Same as Figure 12 with Smoothing Every 250 min (50 time steps)

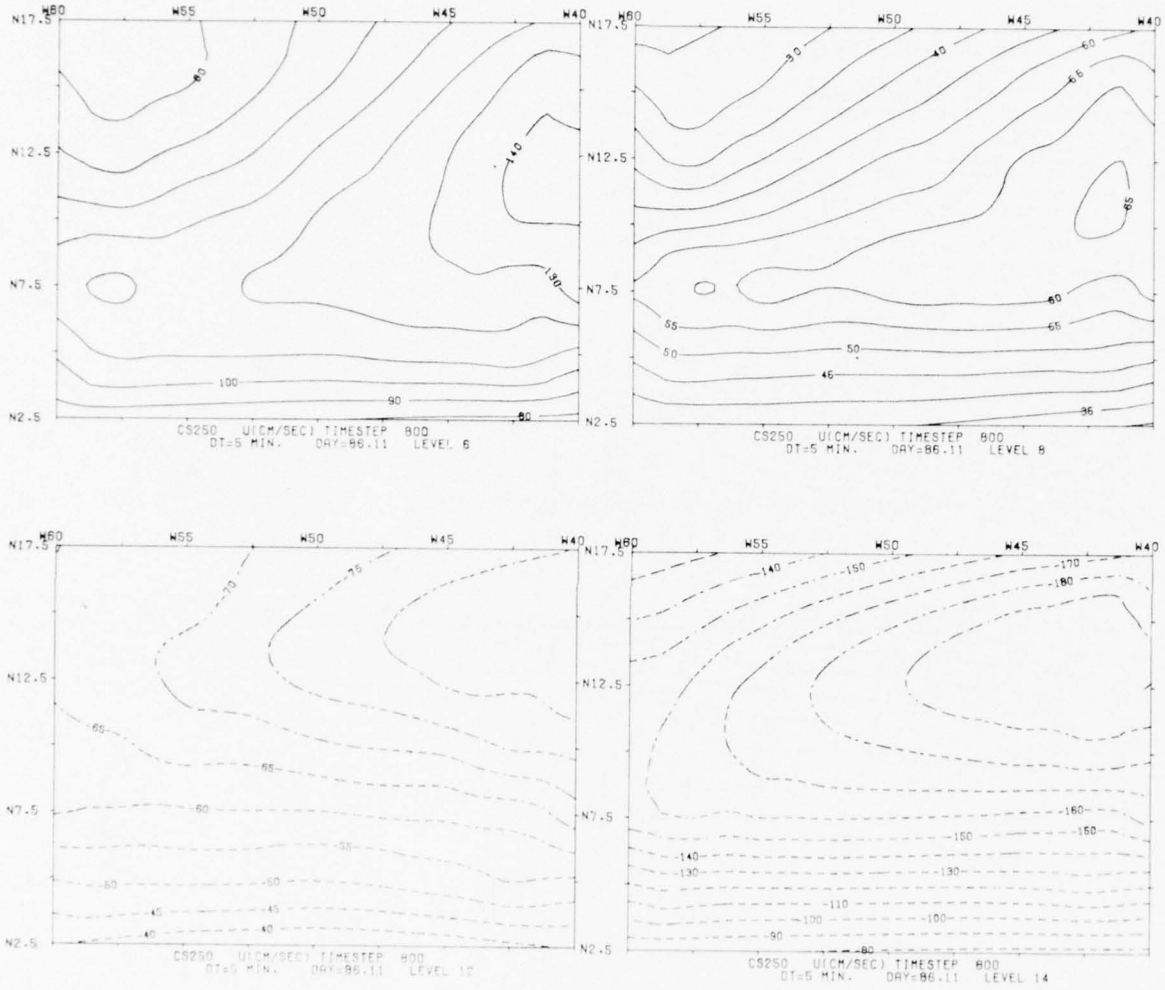

Figure 20. Same as Figure 13 with Smoothing Every 250 min (50 time steps)

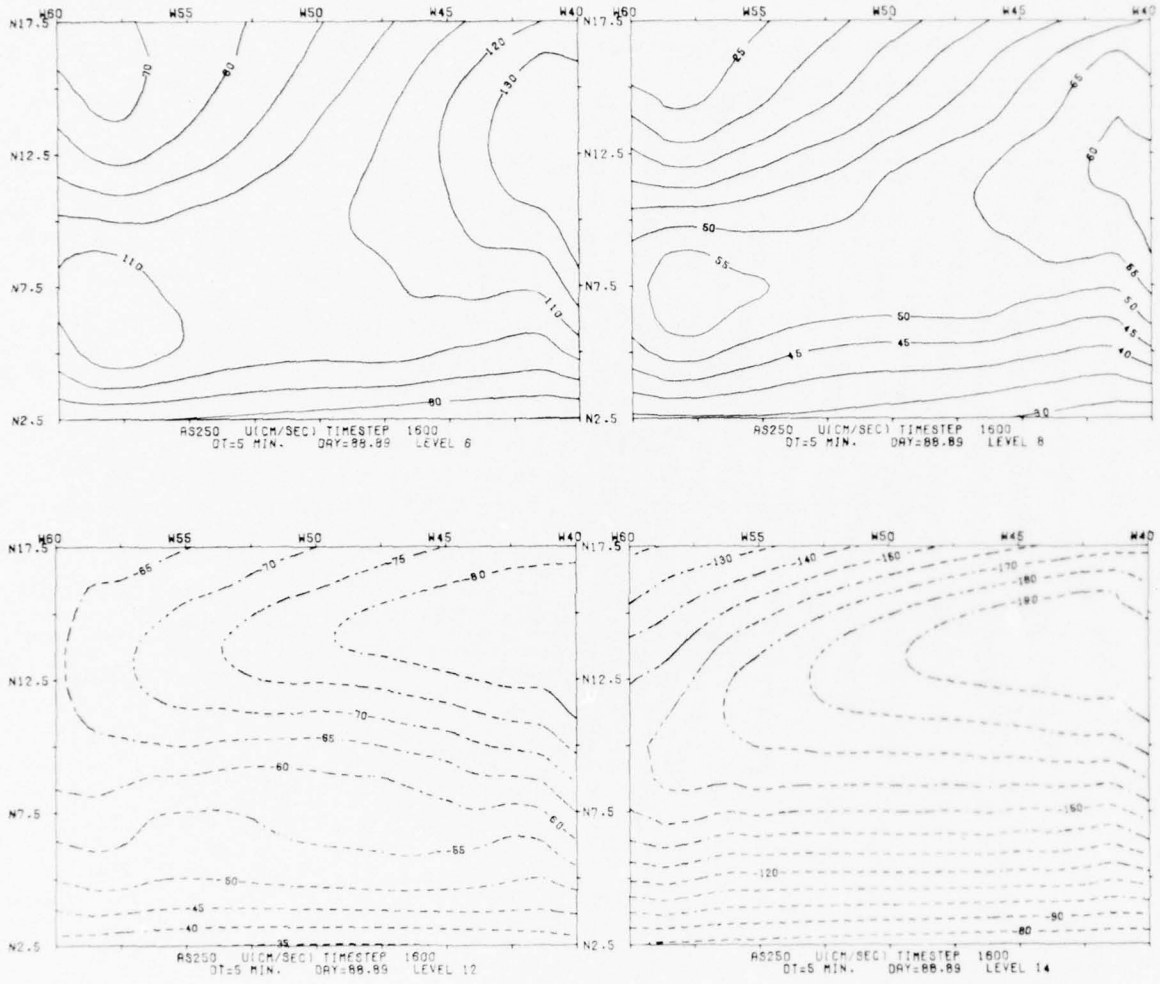

Figure 21. Same as Figure 15 with Smoothing Every 250 min (50 time steps)

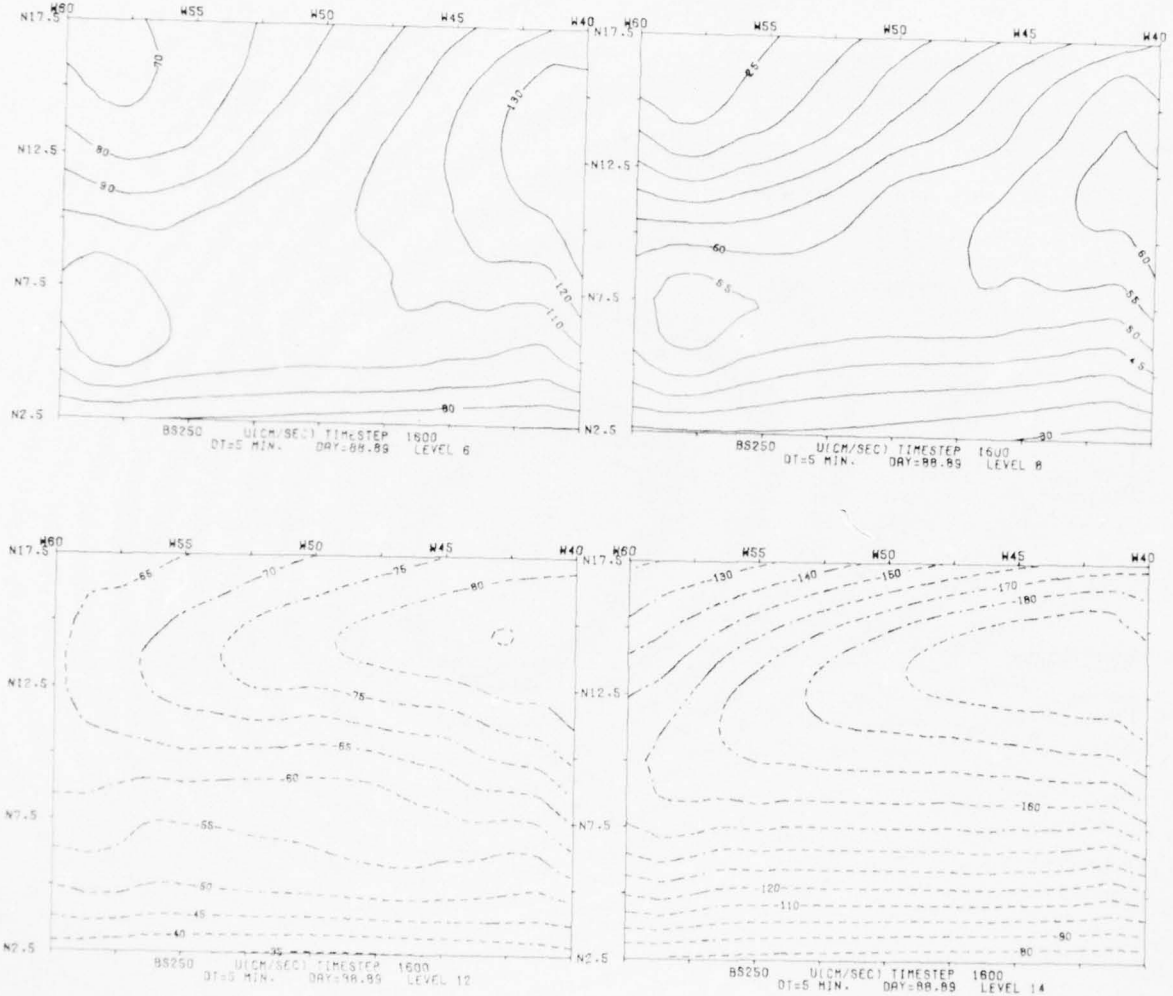

Figure 22. Same as Figure 16 with Smoothing Every 250 min (50 time steps)

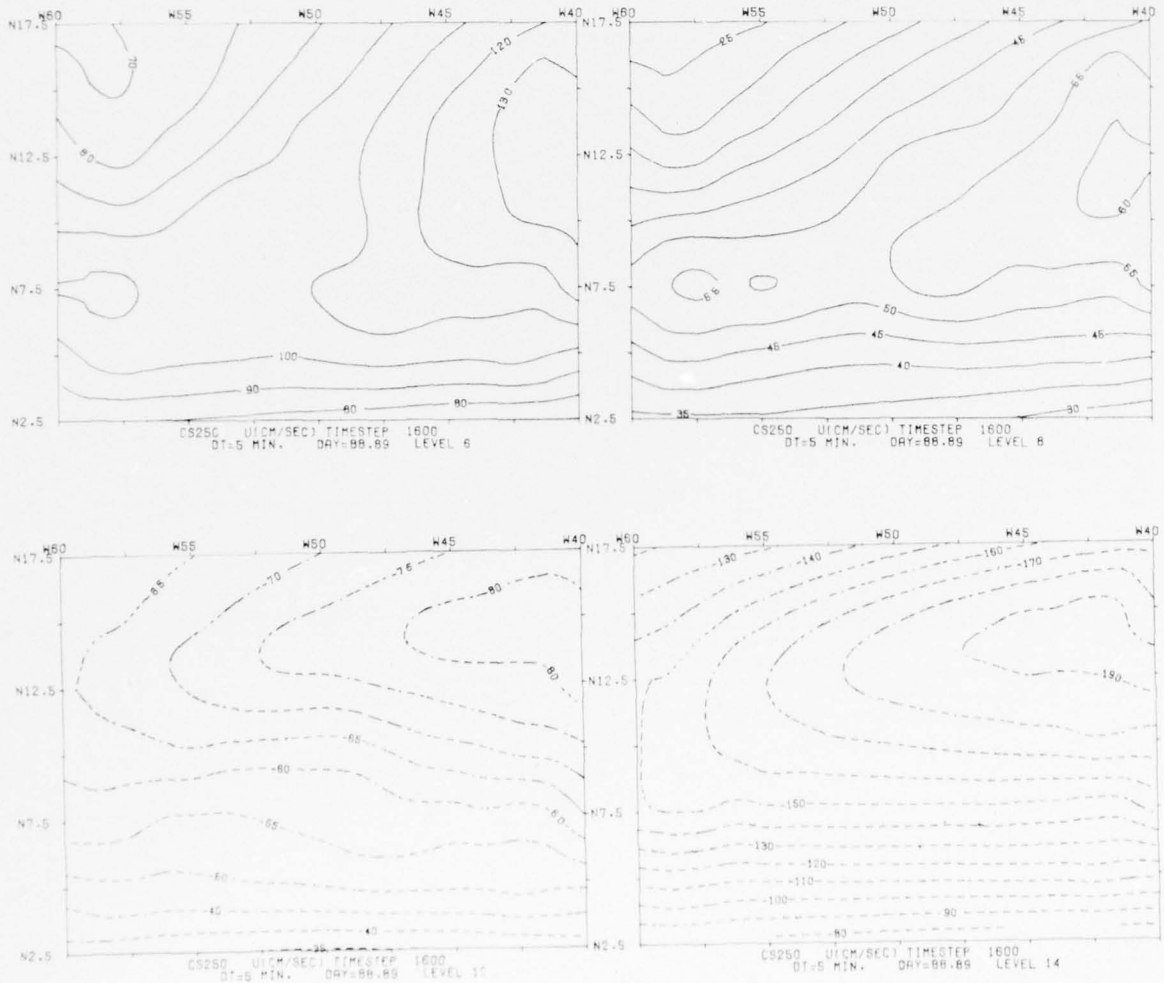

Figure 23. Same as Figure 17 with Smoothing Every 250 min (50 time steps)

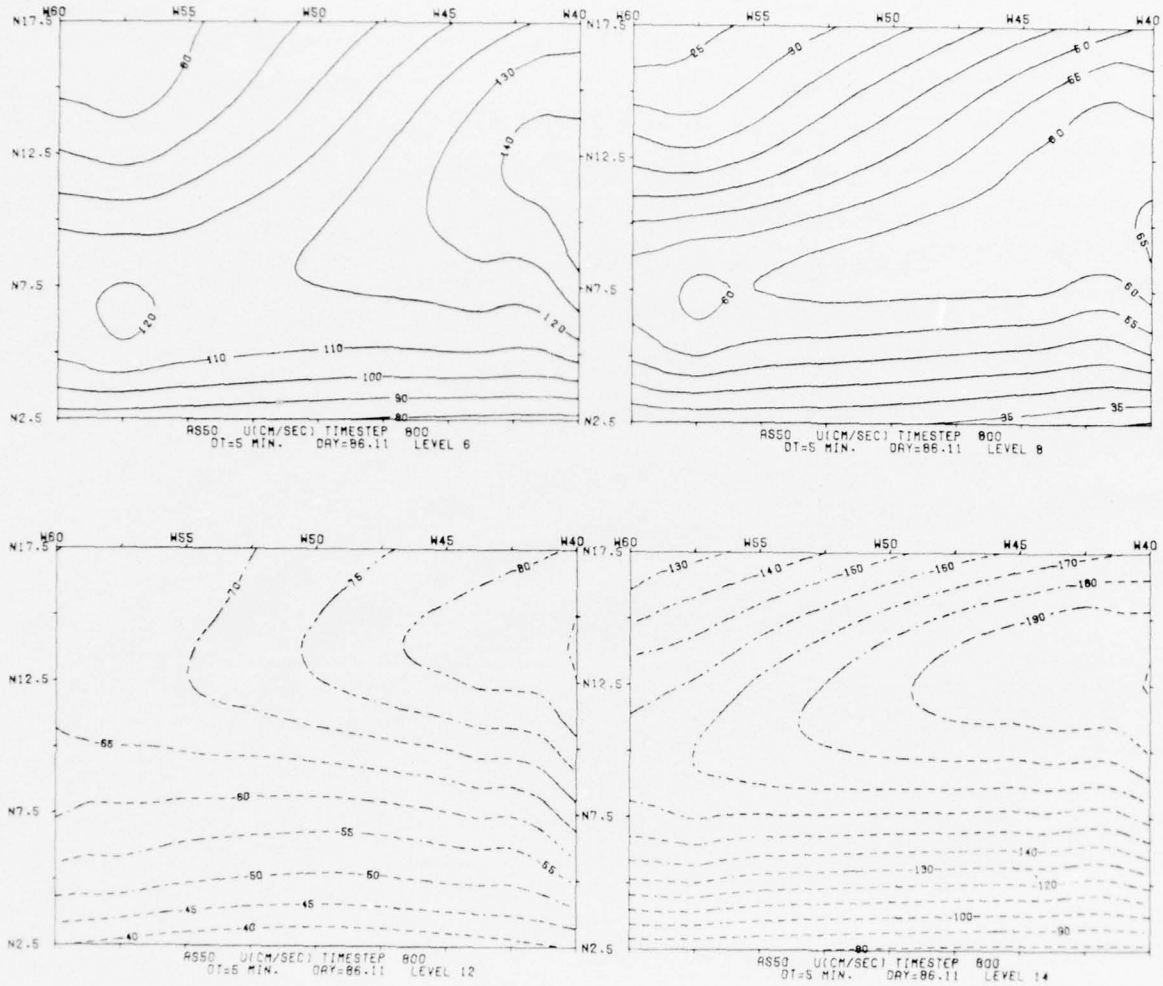

Figure 24. Same as Figure 11 with Smoothing Every 50 min (10 time steps)

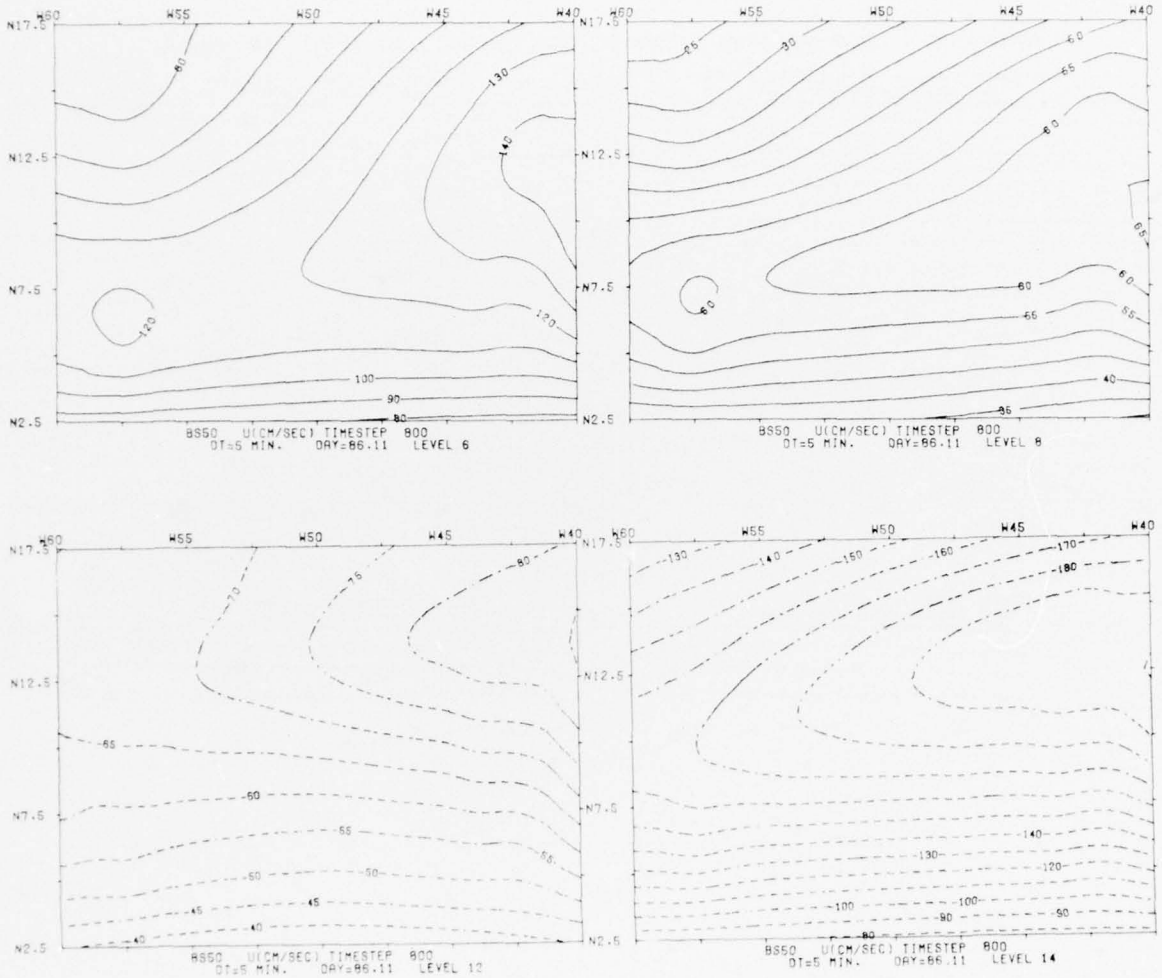

Figure 25. Same as Figure 12 with Smoothing Every 50 min (10 time steps)

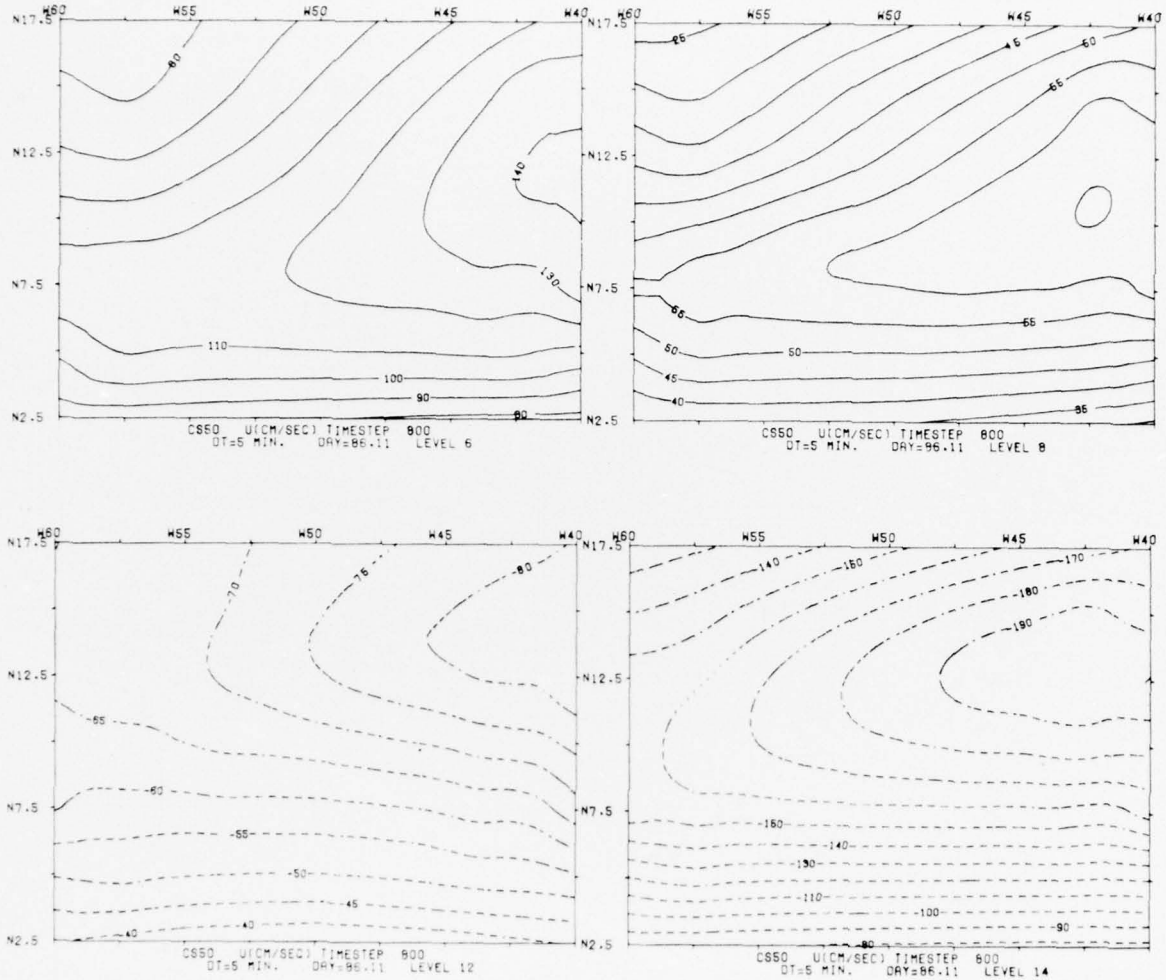

Figure 26. Same as Figure 13 with Smoothing Every 50 min (10 time steps)

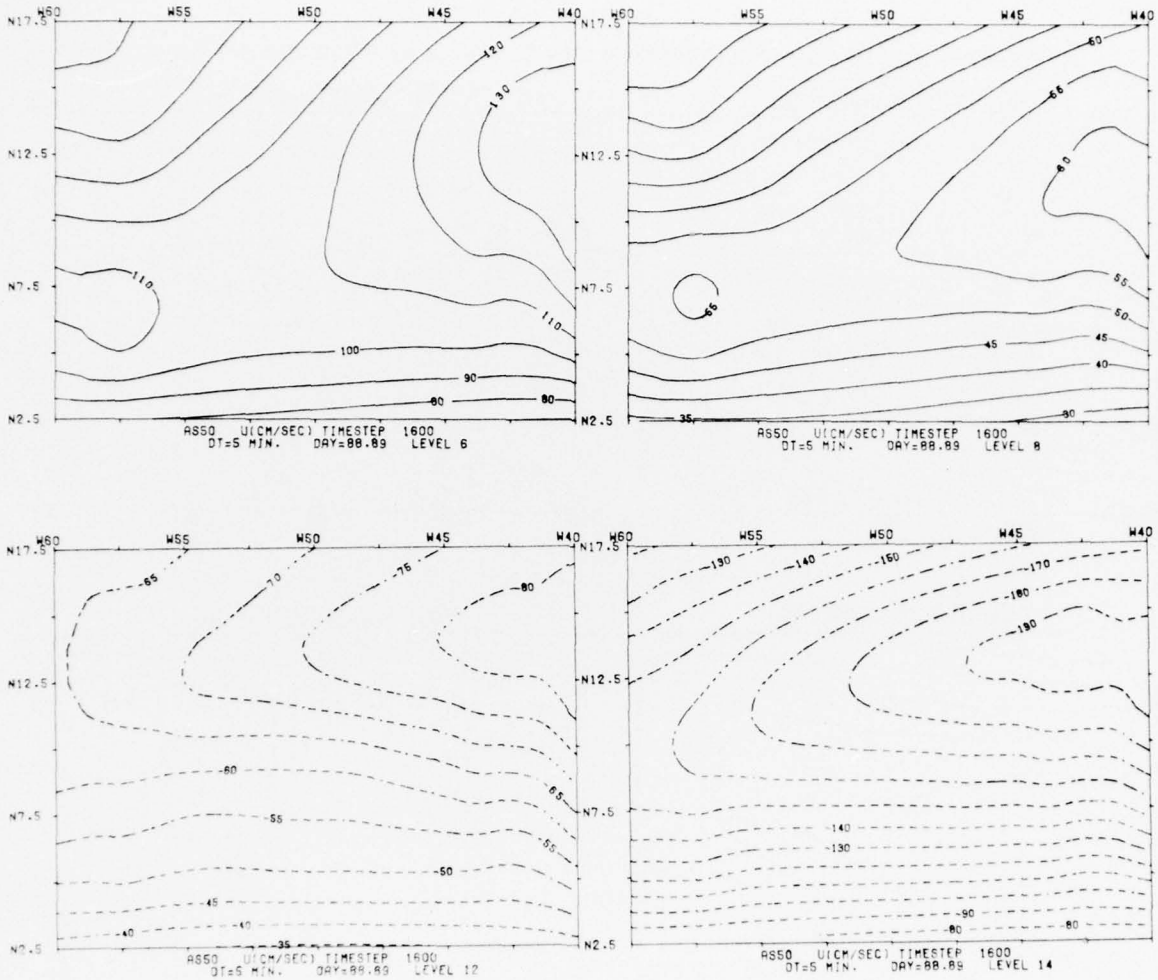

Figure 27. Same as Figure 15 with Smoothing Every 50 min (10 time steps)

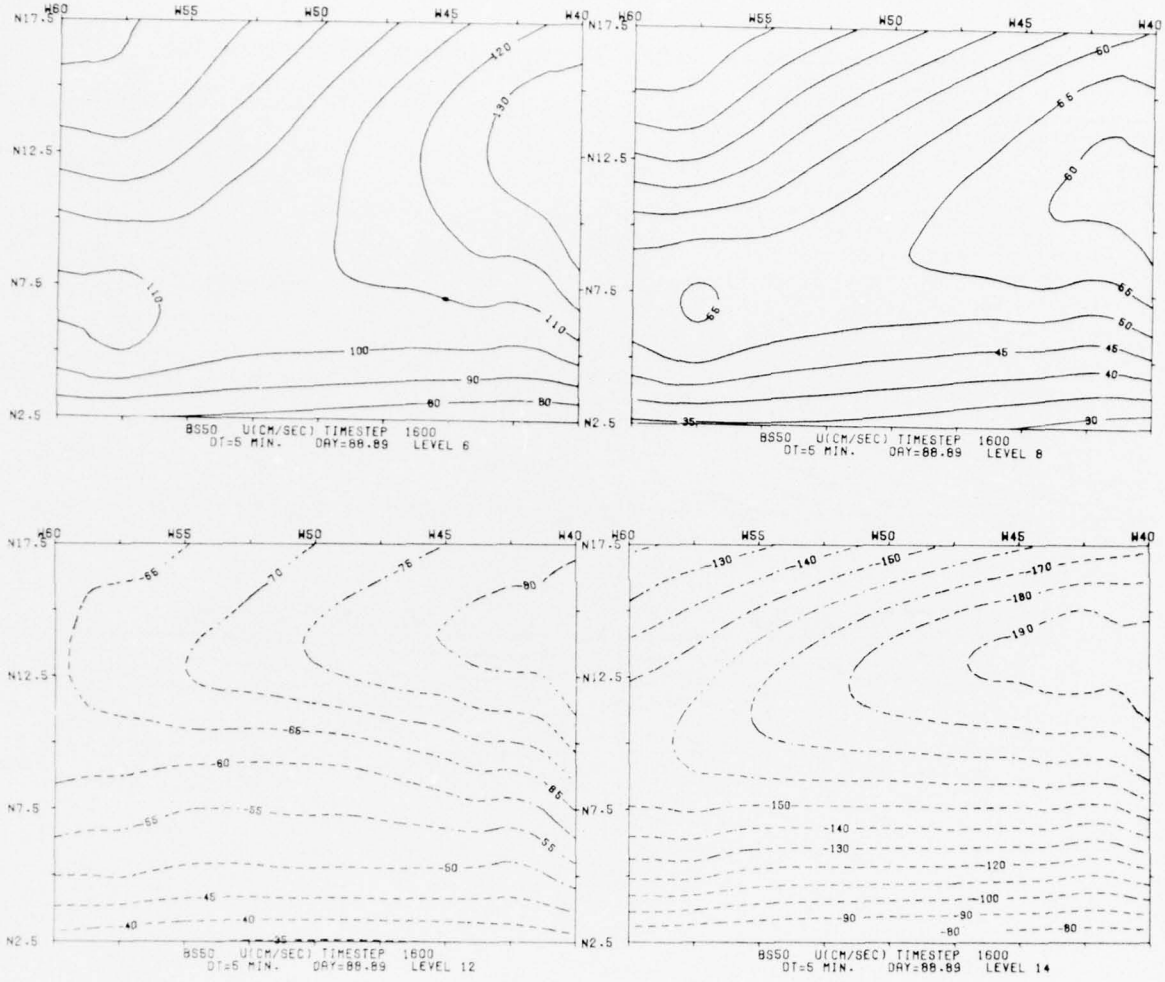

Figure 28. Same as Figure 16 with Smoothing Every 50 min (10 time steps)

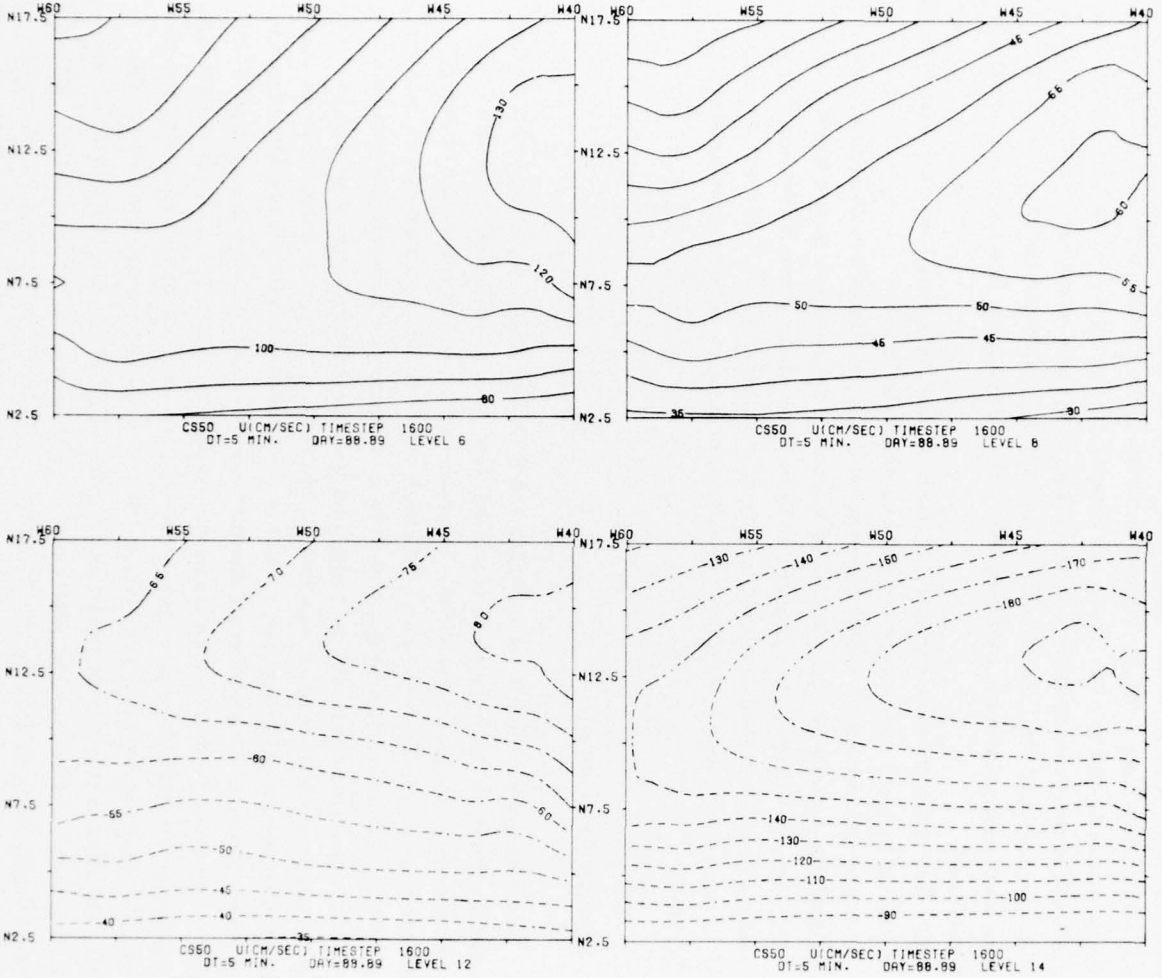

Figure 29. Same as Figure 17 with Smoothing Every 50 min (10 time steps)

Judging from the figures as well as from Tables 3 and 4, all three series generally show some improvement with smoothing every 50 min as compared with those obtained with smoothing every 250 min. However, the differences are rather insignificant except in the case of the RMSD's at level 2. The results for the B Series are generally superior to those of the A and C Series, but here too, the differences are small. It is conceivable, with different initial conditions especially where a greater fraction of the variance is contained in smaller-scale features, that there might have been a larger difference between the results with smoothing every 250 min and every 50 min or among the results for Series A, B, and C. However, the results of the present study in conjunction with those of the earlier study show

(1) that it is of vital importance to control and minimize the phase error that arises from interpolation in obtaining boundary information in a fine-mesh, limited-area solution;

(2) that if the phase error is controlled, a relatively small amount of smoothing is sufficient to yield reasonably smooth and accurate results;

(3) that the amount of smoothing necessary to yield smooth and accurate results depends directly on the care taken to control phase error on the boundaries;

(4) that, therefore, it is preferable to control phase error on the boundaries by using a fine-mesh grid size that maintains a ratio of $(1/2)^n$ of the coarse-mesh grid in conjunction with a relatively simple interpolation scheme such as was used in Series A.

4. ADDITIONAL RESULTS

It had been noted that by day 88.89, the FMV solution develops a small-scale variation that does not develop in any of the test solutions (Series A, B, or C) or for that matter, in the coarse-mesh solution that is used to supply the boundary information for the test solutions. Although the FMV solution remains smooth on day 88.89, it is possible that the small-scale feature is a numerically generated artifact rather than the result of a physical process that becomes manifest in FMV only because of the increased resolution. To help resolve this uncertainty an additional experiment was performed. A new FMV solution was obtained with smoothing every 250 min. A comparison between the new FMV 250 and the original FMV 2000 is shown in Tables 3 and 4 under the column heading FMV 250. It is apparent from the small RMSD's and the large correlation coefficients that the solutions are virtually identical. It is also apparent from Figures 30 and 31, which show the FMV 250 results that are comparable to the FMV 2000 results of Figures 10 and 14, that there is scarcely any noticeable difference between the solutions. It thus seems highly unlikely that the small-scale variation in FMV on day 88.89 is a numerical artifact, since such artifacts typically develop first in the shortest wavelengths which would have been severely dumped by the more frequent smoothing.

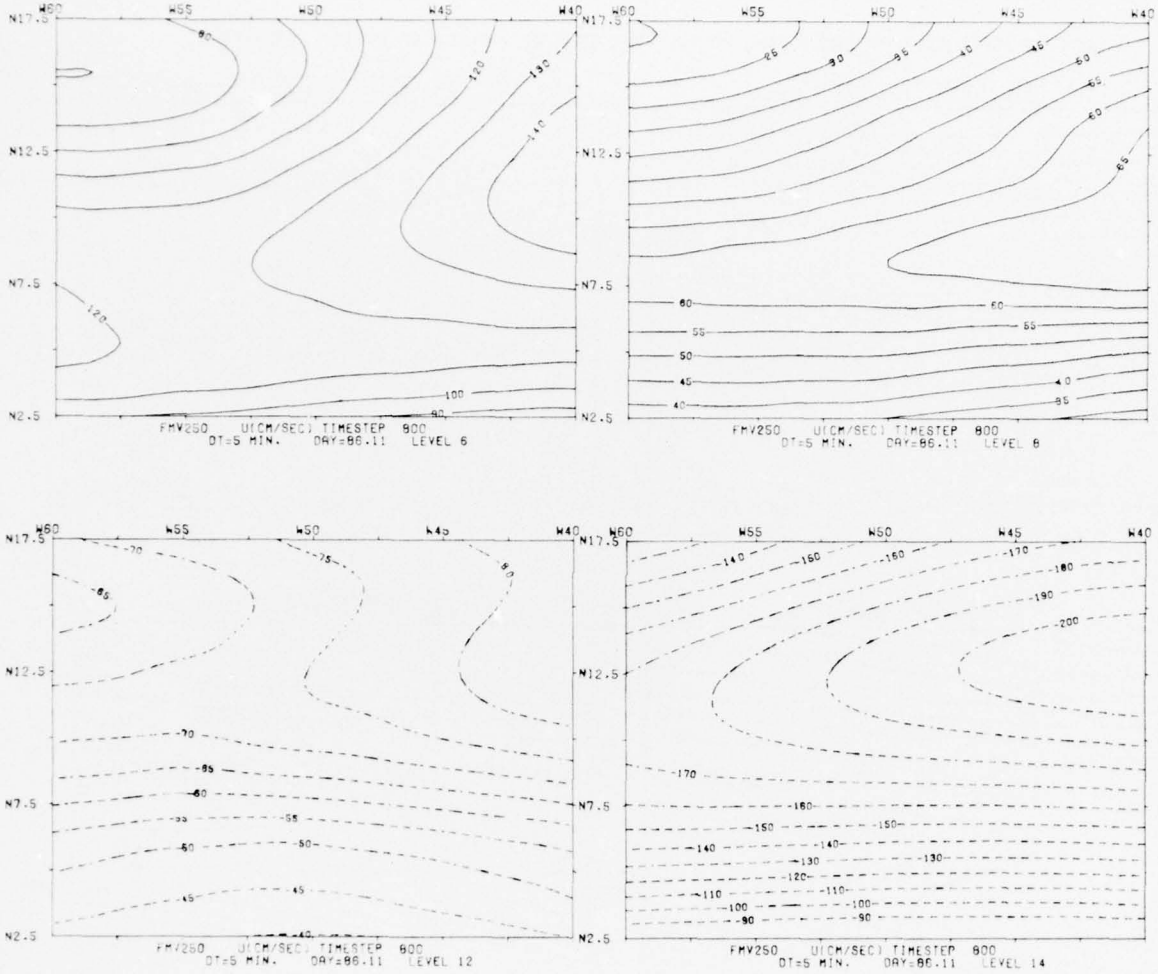

Figure 30. Same as Figure 10 with Smoothing Every 250 min (50 time steps)

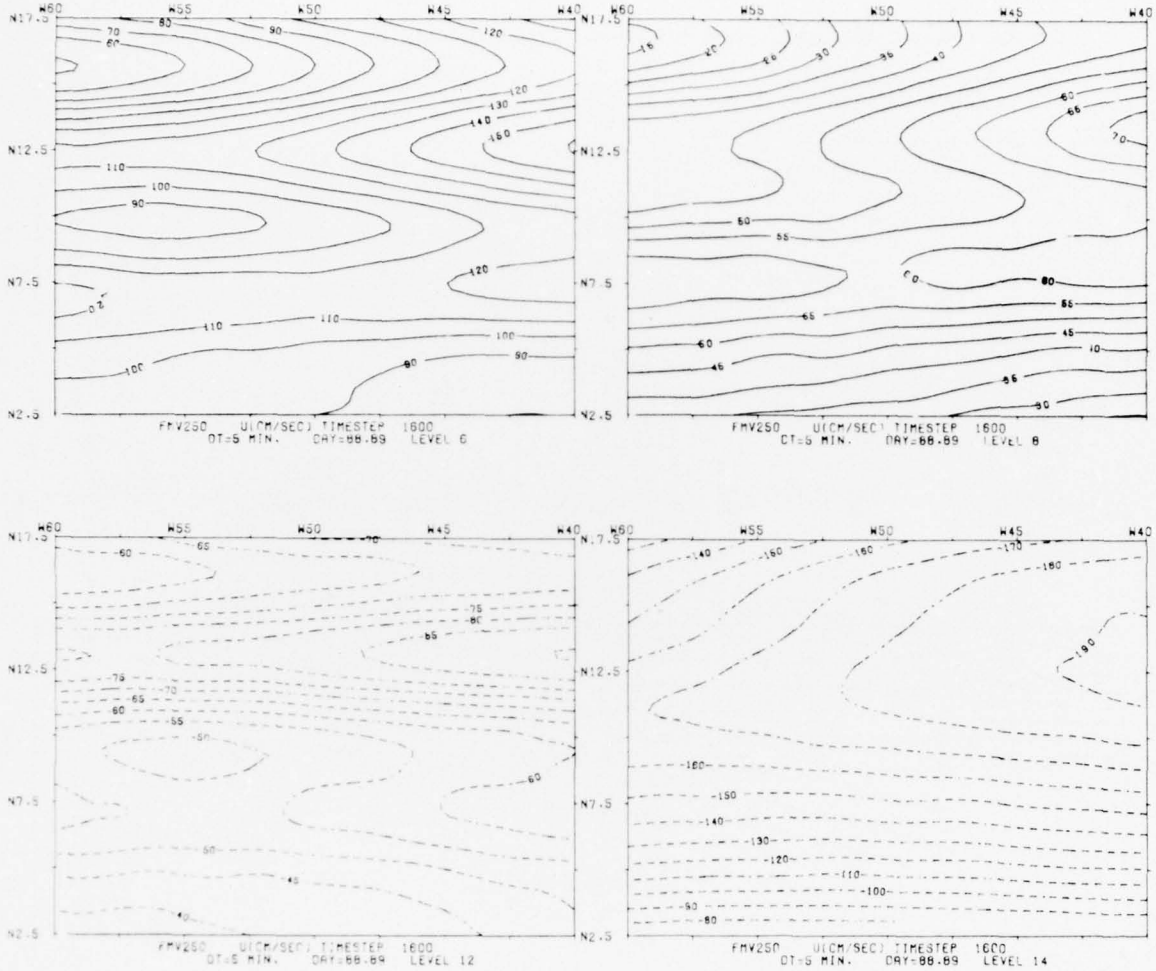

Figure 31. Same as Figure 14 with Smoothing Every 250 min (50 time steps)

5. CONCLUSIONS

The simple, pragmatic procedure proposed here, namely, overspecification of the artificial lateral boundaries of the limited-area domain, in conjunction with (1) care to ensure that approximately correct phase information is supplied to the boundaries, and (2) a weak but high-order smoothing operation, appears to yield satisfactory fine-mesh limited-area solutions in a nested region both in terms of controlling noise and affording verisimilitude to a fine-mesh validation solution. Because of the simplicity of the procedure it appears to have applicability to operational, fine-mesh, limited-area models. However, the results also indicate that unless more information is contained in the initial data of the limited area than is available solely from the large-scale, coarse-mesh model, the fine-mesh solution is not likely to differ appreciably from what would have been obtained from the coarse mesh alone.

References

1. Bushby, F.H., and Timpson, M.S. (1967) A 10-level atmospheric model and frontal rain, Quart. J.R. Met. Soc., 93:1-17.

2. Birchfield, G.E. (1960) Numerical prediction of hurricane movement with the use of a fine grid, J. Meteor., 17:406-414.

3. Moretti, G. (1969) Importance of boundary conditions in the numerical treatment of hyperbolic equations, The Phys. of Fluids Supplement II. High-Speed Computing in Fluid Dynamics, Am. Inst. Phys., N.Y., pp II-13 to II-20.

4. Harrison, E.J., Jr., and Elsberry, R.L. (1972) A method for incorporating nested finite grids in the solution of systems of geophysical equations, J. Atmos. Sci., 29:1235-1245.

5. Koss, W.J. (1971) Numerical integration experiments with variable-resolution two-dimensional cartesian grids using the box method, Mon. Wea. Rev., 99:725-738.

6. Ookochi, Y. (1972) A computational scheme for the nesting fine mesh in the primitive equation model, J. Met. Soc. Japan, 50:37-47.

7. Phillips, N.A., and Shukla, J. (1973) On the strategy of combining coarse and fine grid meshes in numerical weather prediction, J. Appl. Meteor., 12:763-770.

8. Mathur, M.B. (1974) A multiple-grid primitive equation model to simulate the development of an asymmetric hurricane (Isbell, 1964), J. Atmos. Sci., 31:371-393.

9. Price, G.V., and MacPherson, A.K. (1973) A numerical weather forecasting method using cubic splines on a variable mesh, J. Appl. Meteor., 12:1102-1113.

10. Browning, G., Kreiss, H.-O, and Oliger, J. (1973) Mesh refinement, Math. Comp., 27:29-39.

11. Kreiss, H.-O., and Oliger, J. (1973) Methods for the Approximate Solution of Time Dependent Problems, GARP Pub. Ser. No. 10, 103 pp.

12. Kreiss, H.-O. (1970) Initial boundary value problems for hyperbolic systems, Comm. Pure and Appl. Math., 23:277-298.

13. Gustafsson, B., Kreiss, H.-O., and Sundström, A. (1972) Stability theory of difference approximations for mixed initial boundary value problems, II. Math. Comp., 26:649-686.

14. Elvius, T., and Sundström, A. (1973) Computationally efficient schemes and boundary conditions for a fine-mesh barotropic model based on the shallow-water equations. Tellus, 25:132-156.

15. Sundström, A. (1973) Theoretical and Practical Problems in Formulating Boundary Conditions for a Limited-Area Model, Report DM-9, Inst. Met., Univ. Stockholm; Int. Met. Inst. 24 pp.

16. Serrin, J. (1959) Uniqueness theorems for compressible fluids, Arch. Rat. Mech. Anal., 3:271-288.

17. Chen, J.H. (1973) Numerical boundary conditions and computational modes, J. Comp. Phys., 13:522-535.

18. Platzman, G.W. (1958) The lattice structure of the finite-difference primitive and vorticity equations, Mon. Wea. Rev., 86:285-292.

19. Kreiss, H.-O., and Widlund, O. (1967) Difference Approximations for Initial Value Problems for Partial Differential Equations, Report No. 7, Dept. Computer Sci., Uppsala Univ.

20. Richtmyer, R.D., and Morton, K.W. (1967) Difference methods for initial-value problems, Interscience, 2nd Ed., Wiley and Sons, New York, 405 pp.

21. Charney, J.G., Fjörtoft, R., and von Neumann, J. (1950) Numerical integration of the barotropic vorticity equation, Tellus, 2:237-254.

22. Platzman, G.W. (1954) The computational stability of boundary conditions in numerical integration of the vorticity equation, Archiv. fur Meteor., Geophys. and Bioklim., Ser A, 7:29-40.

23. Charney, J.G. (1962) Integration of the primitive and balance equations, Proc. Int. Symp. on NWP, Tokyo, Nov 7-13, 1960, pp 131-152.

24. Sundström, A. (1969) Stability theorems for the barotropic vorticity equation, Mon. Wea. Rev., 97:340-345.

25. Kreiss, H.-O. (1971) Difference approximations for mixed initial boundary value problems, Proc. Roy. Soc. London, Ser A., 323:255-261.

26. Pearson, R.A. (1974) Consistent boundary conditions for numerical models of systems that admit dispersive waves, J. Atmos. Sci., 31:1481-1489.

27. Orlanski, I. (1976) A simple boundary condition for unbounded hyperbolic flows, J. Comp. Phys., 21:251-269.

28. Williamson, D.L., and Browning, G.L. (1974) Formulation of the lateral boundary conditions for the NCAR limited-area model, J. Appl. Meteor., 13:8-16.

29. Shapiro, M.A., and O'Brien, J.J. (1970) Boundary conditions for fine-mesh limited-area forecasts, J. Appl. Meteor., 9:345-349.

30. Davies, H.C. (1973a) On the lateral boundary conditions for the primitive equations, J. Atmos. Sci., 30:147-150.

31. Davies, H.C. (1973b) On the initial-boundary value problem of some geophysical fluid flows, J. Comp. Phys., 13:398-442.

32. DeRivas, E.K. (1974) Comments "On the lateral boundary conditions for the primitive equations," J. Atmos. Sci., 31:596.

33. Davies, H.C. (1976) A lateral boundary formulation for multi-level prediction models, Quart. J. Roy. Met. Soc., 102:405-418.

34. Bennett, A.F. (1975) Open Boundary Conditions for the Limited Area Forecasting Problem, Report No. 9, The GARP Programme on Numerical Experimentation, A. Robert, Ed., pp 114-115.

35. Shapiro, R. (1973) A High-Order Interpolation Procedure for Use in Fine-Mesh Limited-Area Models, Phys. Sci. Res. Pap., No. 560, AFCRL-TR-73-0543, 24 pp.

36. Shapiro, R. (1972) Information loss and compensation in linear interpolation, J. Comp. Phys., 10:65-84.

37. Chen, J.H., and Miyakoda, K. (1974) A nested grid computation for the barotropic free surface atmosphere, Mon. Wea. Rev., 102:181-190.

38. Shapiro, R. (1970) Smoothing, filtering, and boundary effects, Rev. Geophys. and Space Phys., 8:359-387.

39. Shapiro, R. (1975) Linear filtering, Math. Comp., 29:1094-1097.

B

R

10